Eur. Phys. J. A **22**, 213–230 (2004)
DOI 10.1140/epja/i2004-10045-5

THE EUROPEAN PHYSICAL JOURNAL A

Systematics of deformed states around doubly-magic ^{40}Ca

H. Röpke[a]

Physikalisches Institut der Universität Freiburg, Freiburg i.Br., Germany

Received: 1 June 2004 / Revised version: 25 June 2004 /
Published online: 9 November 2004 –
Communicated by D. Schwalm

Abstract. The low-lying rotational bands of $A = 36$–48 nuclei are consistently explained by starting from the recently discovered, superdeformed intrinsic state of ^{36}Ar as the core, filling successively the first three Nilsson orbits above the Fermi border. The critical single-particle energies were obtained from experimental data as were the residual interactions in the parametrization of Brink and Kerman. Implicit are the rearrangement energies due to configuration-dependent equilibrium deformations. The binding energies of 20 experimental bandheads were used to derive the parameters while another 38 bandheads were subsequently predicted and identified almost completely. The Racavy expression reduced by 20% reproduces or predicts the values of the deformation parameter ε. The empirical Nilsson model amended by γ-vibrational and rotation-aligned bands accounts completely for the multi-particle excitations from the $N = 2$ into the $N = 3$ major shell which are not accessible by shell-model calculations. In the case of ^{40}Ca a spectrum of 42 states below $E_x = 8$ MeV is explained.

PACS. 21.60.Ev Collective models – 21.10.Dr Binding energies and masses – 27.30.+t $20 \leq A \leq 38$ – 27.40.+z $39 \leq A \leq 58$

1 Introduction

The level densities [1] of doubly-magic ^{40}Ca and its neighbours are indicative [2] of very low-lying multi-particle excitations from the $N = 2$ into the $N = 3$ major shell. While modern shell-model calculations [3–8] reproduce the few-particle excitations very faithfully computational difficulties are prohibitively high in the case of multi-particle excitations. A way out of the difficulty has been known for more than thirty years. The lowest-lying multi-particle excitations are connected with prolate distortions [9] of the nucleus and can be grouped into rotational bands. The presence of these bands and their intrinsic structures can be explained by the Nilsson model [9–14]. It is an immediate question whether the combination of shell-model and Nilsson model can provide all the degrees of freedom which govern the structure of nuclei in the transitional region from the *s-d* into the *f-p* shell. An answer seems possible once the Nilsson model approach is pursued systematically, which is the goal of the present paper. The empirical approach to the spherical-shell model with single-particle energies and matrix elements of the residual interaction derived from experimental data, is the illuminating example.

The theoretical foundation of an empirical approach to the Nilsson model has been laid in the work of Brink and Kerman [15] who provided an easy-to-handle parametrization of the residual interaction. The experimental prerequisites are equally given today. Most important in this context is the recent observation of a superdeformed $K^\pi = 0^+$ rotational band in ^{36}Ar [16] with $\varepsilon = 0.44 \pm 0.03$ and a bandhead energy of 4329 keV. The large value of the deformation parameter guarantees prolate distortions in heavier nuclei up to ^{48}Cr (or even beyond). The underlying mechanism is explained in fig. 1. This figure gives a slightly schematic diagram of those Nilsson orbits which degenerate into the lowest-lying shell-model state with principal quantum number $N = 3$ or, respectively, the highest-lying state with $N = 2$. Secondary minima of the total nuclear energy develop in regions of deformation where a downsloping, deformation-driving $N = 3$ orbit has crossed an upsloping, sphericity-driving $N = 2$ orbit. The superdeformed secondary minimum of ^{36}Ar is due to the crossing of the $1/2^-[330]$ and $1/2^+[200]$ orbits. The configuration $(\Omega^\pi)^n$ of the last A-32 nucleons is $(1/2^-)^4$. Starting from this configuration as a core it is possible to generate all low-lying deformed intrinsic states of nuclei up to ^{48}Cr by successive filling of the $1/2^+[200]$, $3/2^-[321]$, and $3/2^+[202]$ orbits. A glance at fig. 1 shows that the correct ordering and spacings of orbits are both of paramount importance and difficult to predict because the downsloping $\Omega^\pi = 3/2^-$ level can have crossed the $\Omega^\pi = 3/2^+$ and even the $1/2^+$ orbits at core deformation.

[a] e-mail: muehelga@uni-freiburg.de

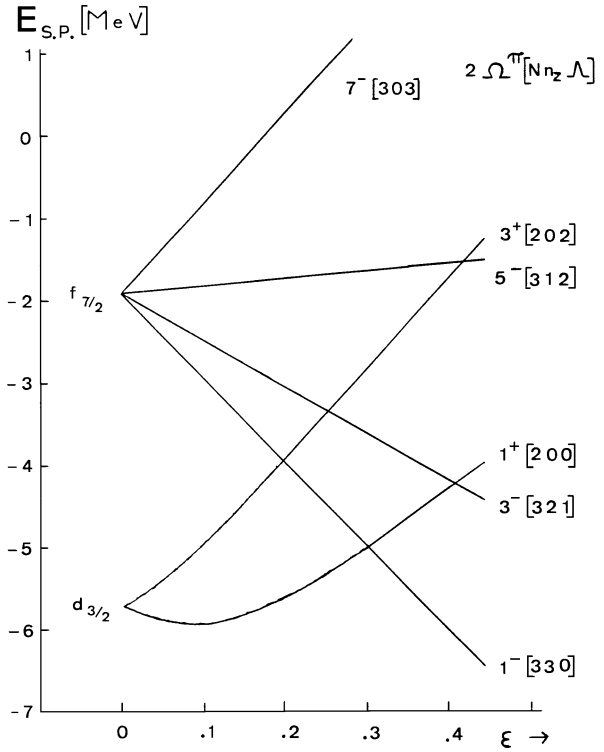

Fig. 1. A schematic drawing of the Nilsson orbits which are of relevance for the nuclides of the ^{40}Ca region. The orbit crossings and the energy scale are adopted from [19].

The role of the $\Omega^\pi = 3/2^-$ orbit was scarcely taken into account in previous work since smaller deformations were considered. Large distortions observed in the established $K^\pi = 0^+$ rotational bands of ^{42}Ca [17] and ^{40}Ar [18] more than 20 years ago can, however, be connected with the first level crossing and the recently discovered superdeformed $K^\pi = 0^+$ band of ^{40}Ca [19] with the second crossing.

It is the goal of the present work to derive an empirical Nilsson model based on an ^{36}Ar core plus up to 12 valence nucleons distributed over three active orbits. A unified description seems possible of all rotational structure from the region of coexisting spherical and deformed states around doubly-magic ^{40}Ca, right into the middle of the $f_{7/2}$ (sub)shell, where deformation is already present in the ground states. The program requires an extended analysis of experimental data and will lead to numerous new identifications of rotational structures. Simultaneously, evidence in favour of γ-vibrational and rotation-aligned bands will emerge. The present paper is organized as follows. The second section provides the theoretical framework needed for the construction of a Nilsson model phenomenology. The Brink and Kerman [15] parametrization of the residual interaction is referred to as is Racavy's method [20] of calculating equilibrium deformations. The third section furnishes the experimental data which serve to determine the parameters of the model. The fourth section is devoted to the calculation of binding energies and deformation parameters of the energetically most favourable Nilsson model configurations in the $N \geq Z$ nuclides between ^{36}Ar and ^{48}Cr. The experimental counterparts of predicted bandheads as far as they are not known yet from sect. 3, are identified, except for the case of the insufficiently investigated doubly-odd nucleus ^{42}K. The fifth section yields an assessment of the theoretical results. A completion of rotational structures by γ-vibrational and rotation-aligned bands is discussed in sect. 6 before a summary is given. The experimental situation for $A = 40$ is analyzed in two appendices and new information on deformed multiparticle-multihole excitations is derived.

2 Theoretical background and definitions

Deformed intrinsic states with axial symmetry yield rotational bands with projection quantum number K. The excitation energies $E_x(J,K)$ of levels are composed under neglect of Coriolis couplings, of a rotational part and an energy $E_x(I)$ of the intrinsic state. The connection is given by

$$E_x(I) = E_x(J,K) - \hbar^2\big(J(J+1) - K^2\big)/2\Theta\,. \qquad (1)$$

Corrections due to the decoupling effect in $K = 1/2$ bands are negligible throughout this work and omitted. In the rare cases of $K = 0$ bands with members of both even and odd spin $E_x(I)$ has to be evaluated separately with use of even- or odd-spin states only and the average be taken.

The "excitation energy" $E_x(I)$ of the intrinsic state can be converted into a binding energy E_B relative to the core, which is to be identified here with the 4329 keV, $J^\pi = 0^+$ state of ^{36}Ar. This binding energy is decomposed in eq. (2) first into a nuclear and a Coulomb part and second into contributions from valence nucleons in identical or different Nilsson orbits. With n_i and m_i being the number of nucleons or, respectively, protons in orbits i, binding energies are given by

$$E_\mathrm{B} = \sum_i (n_i - m_i) E^\mathrm{n}_{\mathrm{B},i} + \sum_j m_i E^\mathrm{p}_{\mathrm{B},i} + \sum_{i,k\geq i} V_{i,k} + \sum_i m_i(m_i-1)E_i/2 + \sum_{i,k>i} m_i m_k e_{i,k}\,. \qquad (2)$$

In this equation single-particle energies of protons or, respectively, neutrons in orbit i are denoted $E^\mathrm{p}_{\mathrm{B},i}$ and $E^\mathrm{n}_{\mathrm{B},i}$, Coulomb interaction energies of protons are denoted E_i if the particles reside in identical orbits and e_{ik} if they reside in different orbits. The nuclear part $V_{i,k}$ of the interaction energies is parametrisized here according to Brink and Kerman [15]. The interaction energies of two nucleons in the same orbit, coupled to different (intermediate) values K', T' of projection quantum number and isospin, are denoted

$$V_{i,i} = \begin{cases} A_i\,, \\ B_i\,, \\ C_i\,, \end{cases} \quad \text{for } K',T' = \begin{cases} 0,1, \\ 0,0, \\ 2\Omega_i, 0. \end{cases} \qquad (3)$$

The interaction energies of three or four particles in the same orbit can be expressed by the aggregate energy $S_i = 3A_i + B_i + 2C_i$ as

$$V_{i,i} = \begin{cases} S_i/2, & n = 3, \\ S_i\,, & n = 4. \end{cases} \tag{4}$$

The interaction energy $V_{i,k}$ between two groups of nucleons in different orbits is given by the expectation value of the operator

$$V_{i,k} = a_{ik} n_i n_k + b_{ik} P_i P_k + 4 c_{ik} \vec{T}_i \cdot \vec{T}_k + 4 d_{ik} \vec{Q}_i \cdot \vec{Q}_k\,. \tag{5}$$

The operators $\vec{T}_i$ and $\vec{T}_k$ stand for the total isobaric spin of all particles in, respectively, orbit i and orbit k. P_i and P_k are the added normalized angular momentum projections $\sum \Omega_\alpha/|\Omega_\alpha|$ and $\vec{Q}_i$ and $\vec{Q}_k$ are defined in a similar way as $\sum(\Omega_\alpha/|\Omega_\alpha|)\cdot\vec{t}_\alpha$ with $\vec{t}_\alpha$ being the isospin operators of the particles. The second and the fourth term of eq. (5) will not play a role in the present paper and stretched isospin coupling schemes will ensure that all operators $\vec{T}_i \cdot \vec{T}_k$ can be replaced by eigenvalues. All binding energies are thus linear combinations of the parameters A_i, B_i, C_i, a_{ik}, c_{ik} and the single-particle energies. Vice versa these parameters can be determined analytically from experimental energies.

The present treatment of binding energies neglects interactions which occur between configurations with agreeing quantum numbers K, π, T, provided that a connection by a two-body operator is given. The neglect is justified by large energetical separations of a few MeV. Deviations from the rule are important in ^{40}Ca and will be discussed further below.

The empirical approach to the residual interactions has the advantage that the effect of rearranging equilibrium deformations is automatically included in the binding energies. Suppose that the total energy of the ^{36}Ar core is given by

$$E_\mathrm{c} = E_\mathrm{c}^0 + \alpha(\varepsilon - \varepsilon_0)^2/2 \tag{6}$$

with ε_0 being the equilibrium deformation (defined in Nilsson's stretched oscillator basis [21]) and α the restoring constant which can be estimated as

$$\alpha = (1/6)\sum(N + 3/2)\hbar\omega_0 \tag{7}$$

with the sum running over all core nucleons. If n_i particles are placed into orbits i and if the single-particle energies vary as

$$E_{\mathrm{B},i} = E_{0,i} + \beta_i(\varepsilon - \varepsilon_0), \tag{8}$$

a new equilibrium deformation is obtained and a rearrangement energy

$$E_\mathrm{R} = \Big(\sum n_i\beta_i\Big)^2/2\alpha \tag{9}$$

is gained. It can vary under the present circumstances from negligible to 10 MeV, depending on whether the slopes β_i given later in subsect. 3.3 have equal or opposite signs. The restoring constant α has a value of 227 MeV obtained with $\hbar\omega_0 = 41A^{-1/3}$ MeV. The rearrangement energy is distributed over the parameters A_i, B_i, C_i with contributions $-{\beta_i}^2/\alpha$, the single-particle energies with contributions $-{\beta_i}^2/2\alpha$, and the parameters a_{ik} with contributions $-\beta_i\beta_k/\alpha$.

The equilibrium deformation which is finally achieved can be calculated from the asymptotic quantum numbers of fig. 1 using Racavy's formula [20]. Tailored to the present situation it reads

$$\varepsilon_\mathrm{R} = (3/2)\frac{\sum_p(3n_z - N) - \sum_h(3n_z - N)}{\sum(N + 3/2)}\,, \tag{10}$$

where the sums in the numerator run over the particles in orbits with principal quantum number $N = 3$ and holes with $N = 2$, while the sum in the denominator runs over all nucleons. The Racavy formula is valid in the limit of large deformations. A recent investigation of deformed *s-d* shell nuclei has shown [22] that very reasonable results can be obtained if a renormalization $\varepsilon = 0.8\varepsilon_\mathrm{R}$ is introduced. This recipe will be followed here.

Experimental values of the deformation parameter can be obtained in the standard way [23] from $B(E2)$'s of in-band transitions between levels with spin J_i and J_f by virtue of

$$B(E2) = (5/16\pi)C(J_i 2K\,0|J_f K)^2 {Q_0}^2\,, \tag{11}$$

$$Q_0 = (4/5)ZR^2\varepsilon(1 + \varepsilon/2), \tag{12}$$

with Q_0 being the intrinsic quadrupole moment. The standard value of the nuclear radius $R = 1.2A^{1/3}$ fm will be used. The Weisskopf unit of $E2$ transition rates, frequently cited in the literature, corresponds to a $B(E2)$ of 0.0594 $A^{4/3}$ e^2 fm^4.

3 The experimental basis of the empirical Nilsson model

The first section has introduced the concept of a superdeformed ^{36}Ar core which acts as the parent of deformed states in nuclei up to ^{48}Cr. The binding energies of intrinsic states relative to the core cover the range from a few to more than hundred MeV with roughly equal contributions from single-particle energies and residual interactions. In the second section semiempirical methods of calculating these energies have been described. For this purpose a set of rotational bands with suitable and safe configurations of the intrinsic state must be provided which can serve to determine the parameters of the theory. The data which are to be discussed in the following are arranged as to allow the stepwise calculation of parameters by elementary means. The first subsection deals with bands used to obtain the single-particle binding energies of eq. (2). This makes a complete analysis of the $T = 1/2$ spectra in $A = 37$ and 41 necessary. The second subsection deals with the bands or intrinsic states which specify the parameter of the residual interactions. About sixty percent of these bands are known but frequently they lack a correct

Table 1. The energy levels of $A = 37$, $T = 1/2$[a].

^{37}Ar		^{37}K			Shell model		
E_x [MeV]	$2J^\pi$	E_x [MeV]	$2J^\pi$	log ft	$2J^\pi{}_v$	E_x [MeV][f]	log ft[k]
0	3^+	0	3^+	5.1	$3_1{}^+$	0	4.99
1.410	1^+	1.371	1^+	5.69	$1_1{}^+$	1.586	5.37
1.611	7^-	1.380	7^-		$7_1{}^-$	1.193	
2.217	7^+	2.285	$7^+(5^+)$		$7_1{}^+$	2.128	
2.491	3^-	2.170	3^-		$3_1{}^-$	2.814	
2.796	5^+	2.750	5^+	4.76	$5_1{}^+$	2.884	4.5
3.171	5^+	3.240	5^+	4.82	$5_2{}^+$	3.112	5.0
3.185	9^-	2.967			$9_1{}^-$	2.814	
3.274	5^-	3.082	5^-		$5_1{}^-$	3.076	
3.518	3^-	3.314	3^-		$3_2{}^-$	4.082	
3.527	7^-	3.272			$7_2{}^-$	3.404	
3.602	3^+	3.622	3^+	4.91	$3_2{}^+$	3.539	4.75
3.707	11^-	[c]			$11_1{}^-$	3.499	
3.937	3^+	3.498			$3_3{}^+$	2.98	
3.980	1^+[b]	3.840	$(1\text{–}5)^+$	4.82[g]			
4.021	9^-	[c]			$9_2{}^-$	4.700	
4.191		3.962					
4.283	7^-	4.127			$7_3{}^-$	4.518	
(4.318)		4.500	1^+	5.01[h]	$1_2{}^+$	4.33	
4.396	5^-	4.191	1–5	6.49[d]	$5_2{}^-$	4.695	
4.444	1^-	4.008	1^-		$1_1{}^-$	4.510	
4.573	$3, 5^+$	4.412	$(1\text{–}5)^+$	5.16			
4.624	7^+	4.732	7^+		$7_2{}^+$	4.685	
4.634	3^-	4.278					
4.743	7^+	4.413	7^+		$7_3{}^+$	4.61	
4.799	$3^+, 5$	4.432	3^+		$3_4{}^+$	5.09	
4.887	7^-–15^-	[c]			$11_2{}^-$	4.718	
4.981	$7^-, 11^-$	4.676	3^-–9^+[e]		$7_4{}^-$	5.184	
5.048	5^-	4.738					
5.090	1^-	4.584	1^-		$1_2{}^-$	5.089	
5.102	$3, 5^+$	4.815	5^+		$5_3{}^+$	5.09	
5.130	$3^+, 5^+$	4.842	5^+		$5_4{}^+$	5.70	
5.213	11^+	[c]			$11_1{}^+$	5.77	
		5.019	3^+	5.0	$3_5{}^+$	5.091	4.75
		5.120	1^+	4.12[i]	$1_3{}^+$	4.620	4.29
		5.132	5^-[l]		$5_3{}^-$	5.316	
5.346	3^-	5.208			$3_3{}^-$	5.038	
5.408	3^-	5.266	3^-		$3_4{}^-$	5.297	

([a]) All experimental data from [1], if not otherwise stated.

([b]) Most likely spin-parity assignment from [24].

([c]) Formation of this level in $^{36}\mathrm{Ar} + \mathrm{p}$ reactions is supressed by the centrifugal barrier.

([d]) The log ft value is compatible with first forbidden character and negative parity of the final state is thus possible.

([e]) The $2J^\pi = 9^-$, 11^- alternatives, allowed by γ-decay, are rejected because formation of this $^{36}\mathrm{Ar} + \mathrm{p}$ resonance with $\ell = 5$ would be suppressed by the centrifugal barrier.

([f]) Positive-parity states are obtained from [3] or, alternatively [25], if a two-digit accuracy is given. For negative parity see [4].

([g]) Possibly generated by a 18% wave function admixture in amplitude squared from the 5.120 MeV level.

([h]) Possibly generated by a 11% wave function admixture in amplitude squared from the 5.120 MeV level.

([i]) The added $B(GT)$ of the 5.120, 3.840 and 4.500 MeV states would result in log $ft = 3.98$.

([k]) From [26].

([l]) Not to be identified with the mirror analog of the 5048 keV, 5^- state of ^{37}Ar which is expected some 300 keV below.

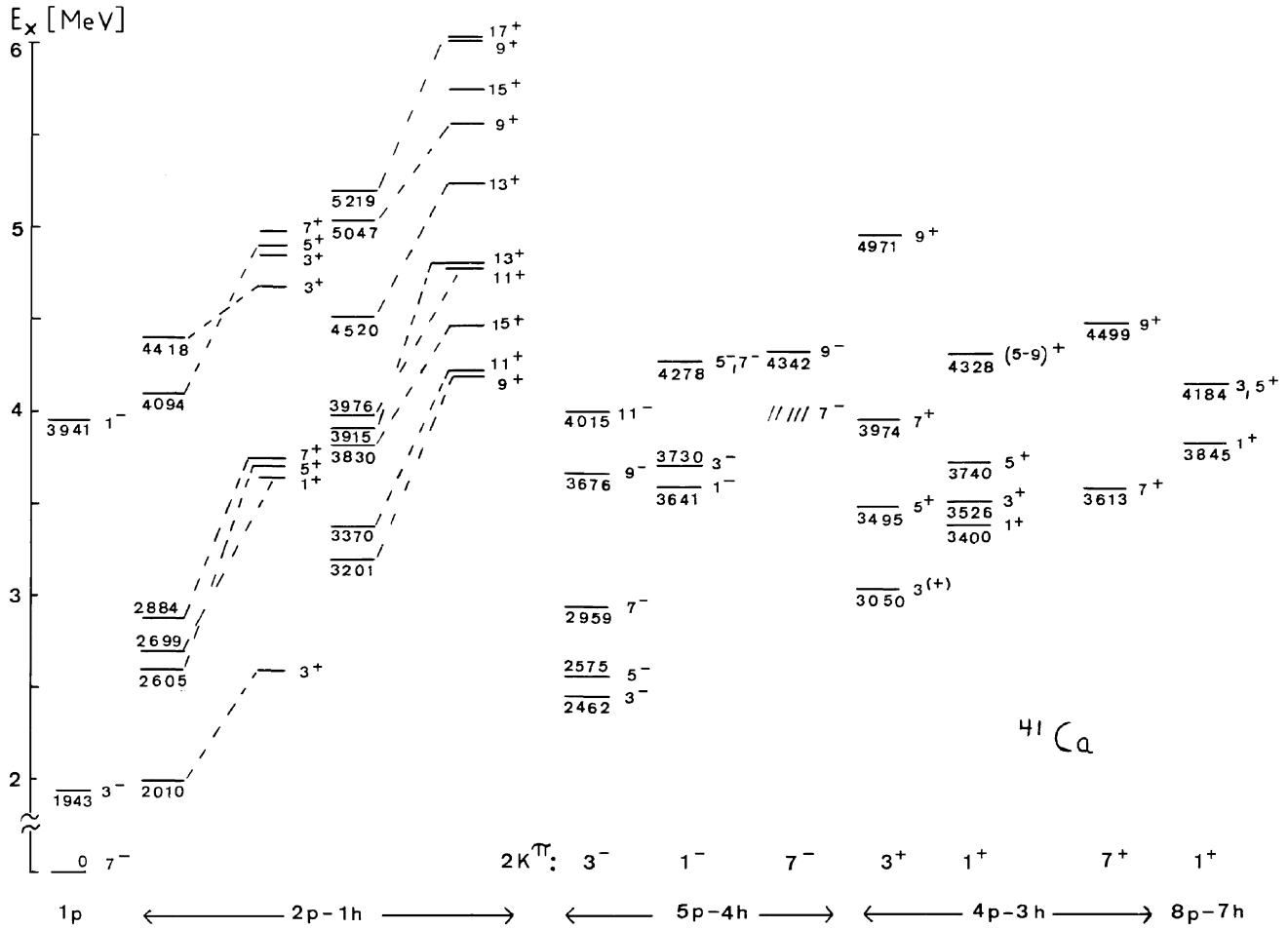

Fig. 2. Interpretatoin of the $T = 1/2$ states in ^{41}Ca. All $E_x < 4.52$ MeV states [1] are displayed amended by a $J^\pi = 7/2^-$ state, the existence of which, at 4030 ± 100 keV, can be inferred from the mirror nucleus. Also given are the $J \geq 9/2$ states up to 5.3 MeV including the 5047 keV level which has a $J^\pi = 9/2^+$ mirror analogue in ^{41}Sc. The different columns contain, from left to right, the experimental 1p states, the experimental and the shell-model [4] prediction of the 2p-1h states, subdivided for better readability into a low-spin and a high-spin part, and a system of rotational bands. The latter constitute the lowest-lying 4p-3h, 5p-4h, and 8p-7h excitations. The notation of quantum numbers is $2J^\pi$.

interpretation. The rest has to be identified yet. Subsections 3.1 and 3.2 are thus playing the additional role of a review of the experimental situation, so that moderate amendments are necessary only in the subsequent sect. 4. The empirical single-particle energies which are finally obtained are compared in subsect. 3.3 to the predictions of a theoretical level diagram, while the parameters of the residual interaction are compared to the results of a similar analysis for the lower half of the *s*-*d* shell [22] and to the spherical limit [27].

3.1 The spectrum of deformed single-particle states

The spectrum of single-particle states above the Fermi border of the ^{36}Ar core is of paramount interest because it affects or determines the structure of all deformed states between ^{36}Ar and ^{48}Cr. The $T = 1/2$ spectra of the mirror nuclei ^{37}Ar and ^{37}K should contain rotational bands which are based on a single particle in one of these orbits. The Nilsson model configuration of the last A-32 nucleons is accordingly (fig. 1) $(1/2^-)^4(\Omega^\pi)^1$ with $\Omega^\pi = 1/2^+$, $3/2^-$ and $3/2^+$ in whatever ordering. The number of particles with principal quantum number $N = 3$ amounts to four or five while the (spherical) ground-state configuration has none. We are thus dealing with $4\hbar\omega$ or $5\hbar\omega$ excitations rather distant from the yrast line. Not surprisingly the standard way of identifying rotational bands by the observation of their high-spin members has failed. An alternative is the identification of bandheads in a dense spectrum of other states which have their origin in $n\hbar\omega$ excitations with $n < 4$.

The prospects are not bad. The goal of a completely known level scheme can be achieved for the first five MeV in excitation by combining the information from the mirror nuclei ^{37}Ar and ^{37}K. Equally the assignments of quantum numbers to levels has reached a high level of completeness [1]. The interpretation of observed levels in terms of $n\hbar\omega$ excitations of the ground state can be

Table 2. A) Binding energies and interaction energies of nucleons in identical Nilsson orbits. B) Interaction energies of particles in different orbits.

A)

Orbit		Neutron/proton binding energy [keV][a]		Interaction energy [keV][b]				
Ω^π	$[\mathrm{Nn}_z\Lambda]$	$E^{\mathrm{n}}{}_{\mathrm{B},i}$	$E^{\mathrm{p}}{}_{\mathrm{B},i}$	S_i	A_i	B_i	C_i	E_i
$1/2^+$	200	−9176	−2386	−13636	−3177	–	(−2799)	439
$3/2^-$	321	−8602	−2028	−12258	−2611	–	−2490	422
$3/2^+$	202	−7263	−609	−16681	−2322	–	−4053	569

B)

Orbit i		Orbit k		Energies [keV][b]		
${\Omega_i}^\pi$	$[\mathrm{Nn}_z\Lambda]_i$	${\Omega_k}^\pi$	$[\mathrm{Nn}_z\Lambda]_k$	a_{ik}	c_{ik}	e_{ik}
$3/2^+$	202	$1/2^+$	200	−381	724	294
$3/2^-$	321	$1/2^+$	200	−193	704[c]	328
$3/2^-$	321	$3/2^+$	202	−264	396	360

([a]) Relative to the $E_x = 4329\,\mathrm{keV}$ level of ^{36}Ar.

([b]) For definition see text.

([c]) An alternative value of 587 keV is obtained in appendix B which yields a more favourable error propagation in the rare cases of antiparallel isospins.

performed for $n = 0, 1, 2$ with the aid of shell-model calculations [3,4,25], while $3\hbar\omega$ excitations are expected above 13 MeV excitation energy according to weak-coupling calculations [27]. The $4\hbar\omega$ and $5\hbar\omega$ excitations are finally obtained by the principle of exclusion. This program is executed in table 1 where the level schemes of ^{37}Ar and ^{37}K are compared to each other and the shell-model. Also included are experimental and theoretical [26] log ft values of the $^{37}\mathrm{Ca} \rightarrow {}^{37}\mathrm{K}$ β-decay.

The comparison of the experimental states performed under consideration of different energy shifts between mirror analogues of positive and negative parity, leads to a safe level scheme for $A = 37$, $T = 1/2$ for the first five MeV in excitation energy. The ^{37}K levels are seemingly complete up to 5266 keV except for the experimentally unaccessible high-spin states which, however, are known in ^{37}Ar. The ^{37}Ar levels are known up to 5213 keV with the possible exception of the mirror analogue of the 4500 keV, $J^\pi = 1/2^+$ state of ^{37}K. The assigned 4318 keV level of ^{37}Ar is somewhat unsafe.

The theoretical energy levels of table 1 are compiled from various shell-model calculations. The negative-parity states constitute $1\hbar\omega$ excitations obtained from [4]. The positive-parity states are comprised of $0\hbar\omega$ and $2\hbar\omega$ excitations. The former ones are obtained from Wildenthal [3] who has also provided log ft values of the $^{37}\mathrm{Ca} \rightarrow {}^{37}\mathrm{K}$ β-decay [26]. The $2\hbar\omega$ states are read from a graph in the work of Hasper [25] and henceforth cited with a two-digit accuracy only, which, simultaneously, distinguishes them from the $0\hbar\omega$ excitations. The correlation of experimental with theoretical levels at higher excitation energies is supported by the β-decay data. Ideally allowed β-decay of ^{37}Ca should feed the $J^\pi = 1/2^+$, $3/2^+$, $5/2^+$ states of $0\hbar\omega$ origin in ^{37}K only. In practice some mixing of configurations is observed. The most prominent decay to the 5120 keV, $J^\pi = 1/2^+$ state shares some 30% of its Gamow-Teller strength with two levels at 3840 and 4500 keV, which do not belong to the $0\hbar\omega$ spectrum. For more details see footnotes to table 1.

The comparison of the experimental level schemes with the theoretical one reveals a surplus of experimental states which is indicative of $4\hbar\omega$ and $5\hbar\omega$ excitations. The 3980 keV, $J^\pi = 1/2^+$; 4191 keV; 4573 keV, $J^\pi = 3/2$, $5/2^+$ states in ^{37}Ar and their mirror analogues at 3840, 3962, 4412 keV in ^{37}K are believed to constitute the first members of the expected $K^\pi = 1/2^+$ rotational band. The spectrum of negative-parity states gives a surplus of one $J^\pi = 3/2^-$ state between 4.6 and 5.4 MeV excitation energy in ^{37}Ar and of a $J^\pi = 5/2^-$ state between 4.7 and 5.2 MeV in ^{37}K. A choice of the proper intruder states on the basis of the shell-model calculations alone is not possible in view of the 500 keV accuracy of the calculations. The situation becomes unique, if the intruders are to be ordered into a $K^\pi = 3/2^-$ band with a reasonable value of the rotational constant $\hbar^2/2\theta$ around 80 keV. In this case the 4634/4278 keV states of ^{37}Ar/^{37}K constitute the bandhead, followed by the 5048/4738 keV states, a lucky choice as it turns out. With these assignments complete theoretical coverage is achieved of the experimental $A = 37$, $T = 1/2$ spectrum up to 5.2 MeV in excitation, which in turn must be considered complete due to the exact match of the ^{37}Ar and ^{37}K level schemes. No room is left for the predicted $K^\pi = 3/2^+$ band which must be sought at higher energies. The Nilsson orbits above the Fermi border of ^{36}Ar thus occur in the order $\Omega^\pi = 1/2^+$, $3/2^-$, $3/2^+$. Such a situation is encountered in the calculated level scheme of fig. 1 for ε values between 0.3 and 0.4.

Information on the missing $K^\pi = 3/2^+$ band can be obtained from the energy levels of the mirror nuclei ^{41}Ca and ^{41}Sc. Two rotational bands are expected which are based on the configurations $(1/2^-)^4(1/2^+)^4(3/2^-)^1$, $K^\pi = 3/2^-$ and $(1/2^-)^4(1/2^+)^4(3/2^+)^1$, $K^\pi = 3/2^+$. Figure 2 shows that they are in fact present. The energetical ordering is as expected with the $K^\pi = 3/2^-$ bandhead

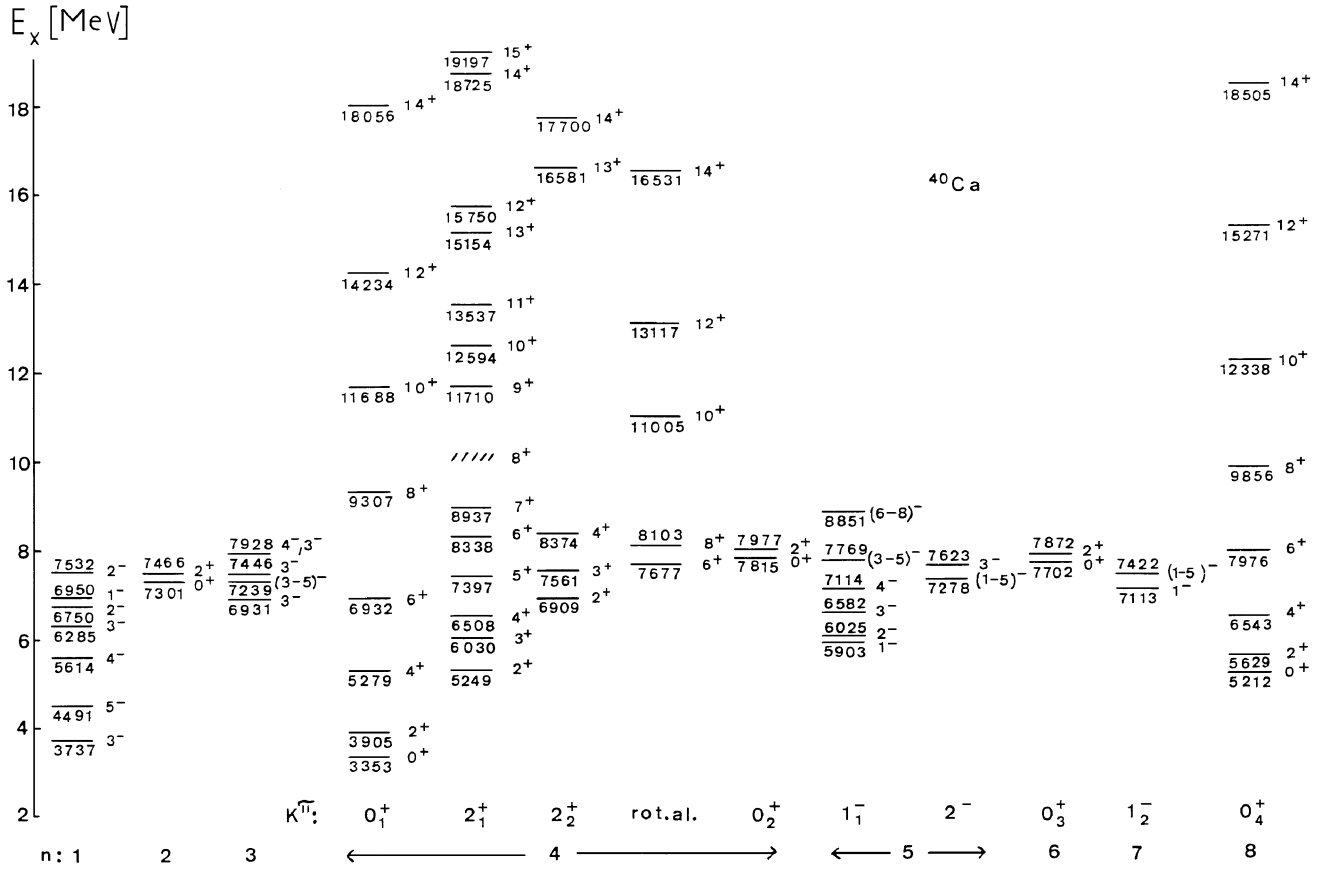

Fig. 3. The excited $T = 0$ states in ^{40}Ca below 8 MeV [1] and the high-spin states below 20 MeV [19] interpreted, from left to right, in terms of spherical states plus rotational bands. Also given is the character of states as $n\hbar\omega$ excitations of the ground state. Parity assignments to the 6931, 7239, 7278, 7422, 7446, 7623, 7769 and 7928 keV states are performed in appendix C. The $K^\pi = 0_1{}^+$, $0_2{}^+$, $0_4{}^+$ bands are discussed in subsect. 3.2.1, the $K^\pi = 2_1{}^+$, $2_2{}^+$, 6^+ bands in sect. 6, the $2\hbar\omega$ excitations in appendix B and the negative-parity states in appendix C.

at 2462 keV (in ^{41}Ca) lying lower than the $K^\pi = 3/2^+$ bandhead at 3050 keV. The spacing is, however, somewhat modified by the interactions of the valence nucleons with the fully occupied $\Omega^\pi = 1/2^+$ orbit which are absent in $A = 37$. The binding energy of a neutron in orbit i relative to a system of core plus completely occupied orbit k is given as

$$E^{n\prime}_{B,i} = E^{n}_{B,i} + 4a_{ik}\,. \tag{13}$$

The necessary corrections which do not affect the level ordering will be made once the binding energy of the ^{40}Ca core is specified and the parameters a_{ik} of eq. (5) are known. The set of single-particle binding energies as they finally emerge is given in table 2. It is interesting to denote in the present context that the $K^\pi = 1/2^+$ band of fig. 2 which is based on the 3845 keV state will turn out to have the underlying configuration of a single particle, coupled to a superdeformed ^{40}Ca core, namely $(1/2^-)^4(3/2^-)^4(1/2^+)^1$.

3.2 Towards a residual interaction

The average contribution of residual interactions to the binding energies of deformed intrinsic states ranges around 40% and comes close in importance to the single-particle energies. The Coulomb part of the interactions will be treated in appendix A. The present section is entirely devoted to the nuclear part knowing that Coulomb corrections can always be performed with adequate accuracy. Subsection 3.2.1 deals with the interaction energies of quartets of nucleons in a single Nilsson orbit and with the interactions between two quartets, each in a different orbit. Experimental information on these quantities is provided by the observation of $K^\pi = 0^+$ rotational bands in $A = 4n$ nuclei. In subsect. 3.2.2 binding energies of quartets in a single orbit are decomposed into their two-body contributions. The experimental information stems from the observation of rotational bands with both $T = 0$ and $T = 1$ assignments in $A = 4n + 2$ nuclei. Subsection 3.2.3 is finally devoted to the isospin-dependent part of the residual interactions between particles in different orbits. This part of the interaction determines the structure of neutron- (or proton-) rich nuclei and the experimental information is provided by the observation of $K^\pi = 0^+$ rotational bands in the isotopes ^{38,40,42}Ar. The section terminates with the specification of all relevant parameters of the residual interaction.

3.2.1 Interaction energies of quartets

The present model of a deformed ^{36}Ar core plus valence nucleons in altogether three Nilsson orbits generates seven $K^\pi = 0^+$, $T = 0$ configurations which are characterized by fully occupied orbits, one in ^{48}Cr and three in both ^{44}Ti and ^{40}Ca, each. The experimental binding energies of bandheads can serve to determine the interaction energies S_i (eqs. (3), (4)) of nucleon quartets in a single orbit and the interaction energies $16a_{ik}$ (eq. (5)) of two quartets occupying different orbits.

The ^{40}Ca spectrum (fig. 3) contains two well-established $K^\pi = 0^+$ bands based on, respectively, the 3353 keV, $J^\pi = 0_2{}^+$ and 5212 keV, $J^\pi = 0_3{}^+$ states [19]. The former band is traditionally assigned [9] a configuration $(1/2^-)^4(1/2^+)^4$, while superdeformation in the second band speaks for a configuration $(1/2^-)^4(3/2^-)^4$ with altogether eight particles in deformation-driving orbits. The third band with configuration $(1/2^-)^4(3/2^+)^4$ is still missing. Its head must be sought among the $J^\pi = 0^+{}_{6\text{–}8}$ levels at 7815, 8019 and 8276 keV excitation energy, while the 7301 and 7702 keV, $J^\pi = 0^+{}_{4,5}$ levels are assigned in appendix B to the lowest-lying 2p-2h and 6p-6h configurations, by the way in accordance with [10]. I adopt the 7815 keV level but the choice of an alternative level would affect the present analysis very marginally, only. The energetical ordering of ^{40}Ca bands is the one which would emerge if the single-particle energies in $A = 37$ were playing the decisive role.

This is certainly no longer the case in ^{44}Ti where two bands based on the ground and first excited $J^\pi = 0^+$ state at 1904 keV, have been identified [28,29]. The ground-state band is characterized by a very moderate deformation and is reproduced by shell-model calculations which employ a closed $N = 2$ major shell [4]. In a Nilsson model picture all orbits which emerge from this shell, must be fully occupied yielding a configuration $(1/2^-)^4(1/2^+)^4(3/2^+)^4$. The second band is consequently based on the configuration $(1/2^-)^4(1/2^+)^4(3/2^-)^4$, while the third band with configuration $(1/2^-)^4(3/2^-)^4(3/2^+)^4$ is safely remote, judging from single-particle energies. The head of the latter band is to be sought among the $J^\pi = 0^+{}_{3,4}$ states at 4605 and 4840 keV [1]. The 4605 keV state is chosen here, rather arbitrarily, while the other state is assigned to the $(f\text{-}p)^4$ shell-model configuration which has its second 0^+ state at a theoretical energy of 5065 keV [4]. The ordering of $K^\pi = 0^+$ bands in ^{44}Ti is strongly influenced by the rearrangement energies of eq. (8) which amount (see subsect. 3.3) to 10 MeV for the ground-state band with eight valence nucleons in sphericity-driving orbits and 1 MeV only for the second band with an equal number of particles in sphericity- and deformation-driving orbits.

The nuclide ^{48}Cr, eventually, shows a well-developed ground-state band [30] and the underlying Nilsson model configuration is unambiguously given as $(1/2^-)^4(1/2^+)^4$ $(3/2^-)^4(3/2^+)^4$.

The binding energies of five out of seven $K^\pi = 0^+$ intrinsic states are needed to fix the values of three quartet-interaction energies S_i and of two inter-orbit interactions a_{ik}, while a remaining a_{ik} value follows from the neutron binding energy of the $K^\pi = 3/2^-$ single-particle configuration of ^{41}Ca (see 3.2.1) relative to the first $K^\pi = 0^+$ configuration of ^{40}Ca by virtue of eq. (13). Two pieces of experimental evidence are thus redundant. The ground-state band of ^{48}Cr was not used in the fitting procedure because of an unfavourable propagation of errors. The superdeformed, second $K^\pi = 0^+$ band of ^{40}Ca was left out of consideration because an interpretation as a 6p-6h rather than an 8p-8h excitation of the ground state should not be excluded from the beginning. Values of the parameters S_i and a_{ik} as they are finally derived are given in table 2.

3.2.2 Interaction energies of two particles in a single orbit

The interaction energy S_i of a nucleon quartet in a single orbit i is made up of two-particle interactions according to $S_i = 3A_i + B_i + 2C_i$ where the quantities A_i, B_i, C_i represent the interaction energies connected with the different coupling schemes of angular momentum projection and isospin (eq. (3)). Information on these quantities can be obtained from a study of $A = 4n + 2$ nuclei since the quantum numbers of low-lying rotational bands are due to just one pair of particles. The programme requires a detailed analysis of experimental data and makes this subsection the most extended one of the article. A first estimate of bandhead excitation energies is obtained by assuming $A_i = B_i = C_i = 1/6S_i$. Experience shows weaker binding for $K = 0$, $T = 0$ couplings and the associated bands will in part remain unobserved or tentative. Because of error propagation it makes little sense to derive a missing value of B_i from the values of S_i, A_i, and C_i.

Most important are the interaction energies A_i of particle pairs with $K', T' = 0, 1$ coupling because such pairs constitute the building blocks of configurations with large isospin or neutron/proton excess. A single such pair is responsible for $K^\pi = 0^+$, $T = 1$ rotational bands in ^{38}Ar and ^{42}Ca. According to the simple estimate $A_i = 1/6S_i$ two rotational bands are expected in ^{38}Ar with bandheads at 4.3 and 5.7 MeV excitation energies and underlying Nilsson model configuration $(1/2^-)^4(1/2^+)^2{}_{0,1}$ and $(1/2^-)^4(3/2^-)^2{}_{0,1}$. The subscripts denote the intermediate quantum numbers K', T' which are identical with the final quantum numbers. The first band has been observed long time ago [31] and starts with the 3377 keV, first excited $J^\pi = 0^+$ state. The second band has possibly been observed in a very recent experiment [32]. A series of $J^\pi = 4^+, 6^+, \ldots 14^+$ levels at $E_x = 6054, 7492 \ldots 17003$ keV is connected by $E2$ decay of a yet unknown strength. The 5156 keV, 2^+ and 4700 keV, 0^+ levels are available to complete the band since they do not belong to the s-d shell configuration [3]. A rotational constant $\hbar^2/2\theta$ of 60 keV is indicative of a large deformation and thus in support of an underlying $(1/2^-)^4(3/2^-)^2$ configuration with six particles in deformation-driving orbits.

In the case of ^{42}Ca two $K^\pi = 0^+$ bands are predicted around 2.4 and 3.5 MeV excitation energies, being based on the Nilsson model configurations

$(1/2^-)^4(1/2^+)^4(3/2^-)^2{}_{0,1}$ and $(1/2^-)^4(1/2^+)^4(3/2^+)^2{}_{0,1}$ or in other words having a 6p-4h and 4p-2h character. The first band is well known experimentally, starting with the first excited $J^\pi = 0^+$ state at 1837 keV [17]. A large value $Q_0 = 1245 \pm 180$ mb of the intrinsic quadrupole moment, corresponding to roughly $\varepsilon = 0.35$, speaks for a configuration with six rather than four particles in deformation-driving orbits. The head of the 4p-2h band, which had been predicted at 2 MeV excitation energy in the work of Flowers and Skouras [11], has been located at 3300 keV excitation energy by four-particle transfer with the ^{38}Ar(^{6}Li, d) reaction [33]. The 3654 keV, 2^+ and 5016 keV, 4^+ states of ^{42}Ca are available to constitute the next members of the band because they are not needed to account for the $(f\text{-}p)^2$ shell-model configuration [4].

The interaction energies A_i of table 2 were obtained with use of the ^{42}Ca bands and the first ^{38}Ar band. The results would change only marginally if the role of the first band in ^{42}Ca were being played by the second band of ^{38}Ar.

The interaction energies of two particles in the same orbit coupled to $K', T' = 2\Omega, 0$ can be studied in the doubly-odd nuclides ^{38}K and ^{42}Sc, where rotational bands with just these quantum numbers should exist. The simple estimate $C_i = 1/6 S_i$ leads to the prediction of a $K^\pi = 1^+$ bandhead in ^{38}K at 4.3 MeV excitation energy with underlying Nilsson model configuration $(1/2^-)^4(1/2^+)^2{}_{1,0}$. In ^{42}Sc two $K^\pi = 3^+$ bandheads are expected at 2.4 and 3.5 MeV and configurations $(1/2^-)^4(1/2^+)^4(3/2^-)^2{}_{3,0}$ and $(1/2^-)^4(1/2^+)^4(3/2^+)^2{}_{3,0}$.

An analysis of the ^{38}K level scheme in terms of $(0+2)\hbar\omega$ and $1\hbar\omega$ excitations analogous to the case of $A = 37$ in table 1 had already [34] revealed the presence of a single "intruder" state below 5.2 MeV excitation energy. It has to be sought among the closely spaced $J^\pi = 1^+$ states at 3857 and 3978 keV and constitute a $4\hbar\omega$ excitation. The intruder state, assumed here to be the 3978 keV level, has the properties of the $K^\pi = 1^+$, $T = 0$ bandhead. The alternative interpretation as head of the $K^\pi = 0^+$, $T = 0$ band which is obtained by recoupling of the angular momentum projections, cannot be excluded though this band is expected at higher energy.

The $T = 0$ spectrum of ^{42}Sc is scanned in fig. 4 for rotational structures, following a similar attempt by Flowers and Skouras [11] a generation ago. It appears [1] that the ^{41}Ca(τ, d) reaction has spotted the positive-parity states with $J = 0$–7 by single-particle transfer via fragments of the $1f_{7/2}$ and $2p_{3/2}$ single-particle strengths. Levels at 2269 keV and higher excitation energies which are not reached by transfer reactions are thus believed to have negative parity. This topic is dealt with further below.

In the case of positive-parity states it is easy to locate the spherical states of the $(f\text{-}p)^2$ shell-model configuration by comparison with the calculations of [4]. For the remaining states the attempt of rotational model interpretation is made in fig. 4. Quantum numbers or restrictions thereof allow the construction of a first $K^\pi = 3^+$ and of a $K^\pi = 1^+$ band. The level spacings within the bands are compatible with previous observations in doubly-odd ^{46}V where rotational structures are well investigated [35]. Bandhead character can also be inferred for the 2223 keV, $J^\pi = 2^+, 3^+$ state because the γ-decay of the 2996 keV, $J^\pi = (3\text{–}5)^+$ states feeds [1] the former level with a large branching ratio of 80% in spite of an unfavourably low transition energy. Such behaviour is typical of enhanced inband $E2$ decay. The 2223 keV level will be interpreted as the head of a second $K^\pi = 3^+$ band, while it remains to be seen whether the 2996 keV level constitutes the second member or the third in which case it is necessary to incorporate the 2587 keV level of unknown parity as the second one. Equally open, experimentally, is the question whether the $J^\pi = 1^+$ level at 2222 keV carries a $K = 0$ or a $K = 1$ assignment.

Contrary to the first guesses it is necessary to assign the configuration $(1/2^-)^4(1/2^+)^4(3/2^-)^2{}_{3,0}$ to the second $K^\pi = 3^+$ band and the alternative configuration $(1/2^-)^4(1/2^+)^4(3/2^+)^2{}_{3,0}$ to the first one. This choice meets three requirements simultaneously. The interaction of two particles in the $\Omega^\pi = 3/2^-$ orbit is thus more binding for $K' = 0$, $T' = 1$ coupling than for $K' = 2\Omega$, $T' = 0$ coupling, as required by observations made in ^{46}V [35]. Opposite behaviour can be inferred for two particles in the $\Omega^\pi = 3/2^+$ orbit according to calculations in [11] with use of a Rosenfeld force. The interaction energies C_i for $K' = 2\Omega$, $T' = 0$ coupling deduced in table 2 fulfil both requirements. The strong, -16.7 MeV, binding energy of a nucleon quartet in the $\Omega^\pi = 3/2^+$ orbit finds eventually its explanation in a strong, -4.05 MeV, binding energy between two such particles in the $K' = 2\Omega$, $T' = 0$ state.

The $K^\pi = 1_1{}^+$ band of fig. 4 is present in the calculations of Flowers and Skouras [11] who considered configurations with two or four particles in orbits (whether spherical or deformed) with principal quantum number $N = 3$. The Nilsson model configuration of the $K^\pi = 1_1{}^+$ band is thus almost inevitably $(1/2^-)^4(1/2^+)^3(3/2^+)^3$ and will be subject of further discussion in sect. 6. It is appealing but not hundred percent safe to interpret the $J^\pi = 1^+$ state at 2222 keV excitation energy as the head of a $K^\pi = 0^+$, $T = 0$ band based on the configuration $(1/2^-)^4(1/2^+)^4(3/2^-)^2{}_{0,0}$. The present assignments lead to the two-body interaction energies C_i of table 2 but leave open the values of B_i.

I note in passing that rotational bands of negative parity are known in doubly-odd ^{46}V which are based on a configuration with an odd number of nucleons in each of the $\Omega^\pi = 3/2^-$ and $3/2^+$ orbit [35]. The same system of bands should exist in ^{42}Sc and start at 3 MeV excitation energy according to the theory which is to be developed here. The ^{46}V spectrum is given in column eight of fig. 4, however shifted by the moderate amount of 0.73 MeV as to start at 2.27 MeV. In this way it is possible to account for the rapid proliferation of levels with (alleged) negative parity (column nine) above this energy. The spherical 3p-1h states, predicted by shell-model calculations and contained in column seven, are not able, alone, to account for the level density.

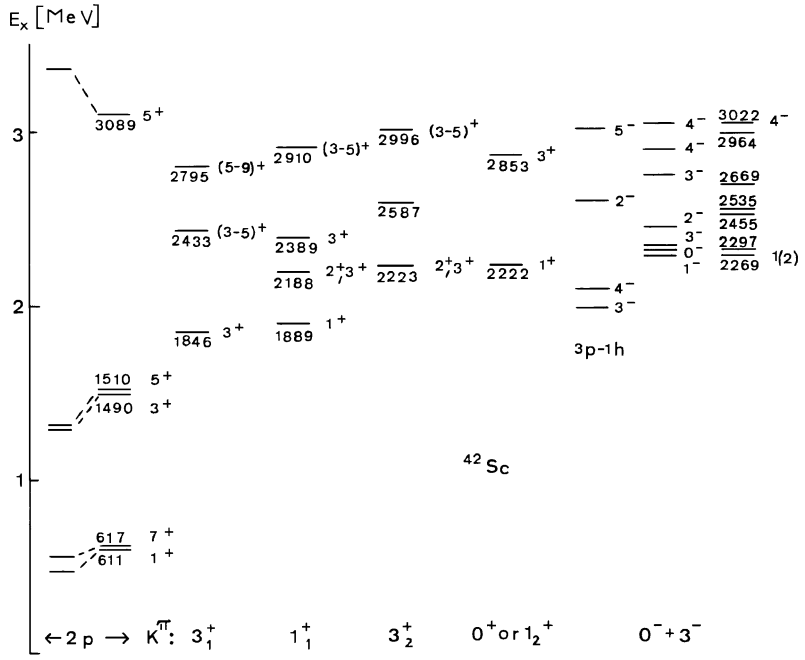

Fig. 4. Interpretation of the $E_x \leq 3022\,\mathrm{keV}$, $T = 0$ states of ^{42}Sc [1]. The figure gives, from left to right, the spherical 2p states as they are predicted [4] and observed, the additional experimental states of positive-parity, grouped into rotational bands, the predicted [4] negative-parity states of 3p-1h character, the deformed negative-parity states as predicted by analogy with ^{46}V (see text), and the remaining experimental levels, all having or being suspect of (see text) negative parity.

3.2.3 Isospin dependences of interactions

The last topic of this section deals with binding energies of neutron- and proton-rich nuclei or, in other words, with configurations of higher isospin. For this purpose two parameters have to be known. The interaction energies A_i of two particles in the same orbit, coupled to $K', T' = 0, 1$ have already been determined. Second in place is the knowledge of the parameters c_{ik} in eq. (5) which govern the isospin dependences of interactions between particles in different orbits. (Use of the additional parameters b_{ik} and d_{ik} of eq. (5) can be avoided here.) In the following, stretched isospin coupling schemes are treated which yield interaction energies $2c_{ik}$ between a single particle in orbit i and a $K', T' = 0, 1$ pair of particles in orbit k, and an energy $4c_{ik}$ for the interaction of two $K', T' = 0, 1$ pairs.

The uncertainties lead, for positive eigenvalues of the operator $\vec{T}_i \cdot \vec{T}_k$ to a reduction of binding-energy errors, as they are induced by the uncertainties of the other parameters. The opposite case of negative eigenvalues and enhanced errors occurs only once in the course of this work. The 6p-6h configuration $(1/2^-)^4(1/2^+)^2{}_{0,1}(3/2^-)^2{}_{0,1}$ of the $A = 40$ system can occur with total isospin $T = 2, 1, 0$ and eigenvalues $\vec{T}_i \cdot \vec{T}_k = 1, -1, -2$. A rather unsafe prediction of the $T = 0$ energies can be improved by identifying first (appendix B) and subsequently using the experimental $T = 2$ and $T = 1$ energies.

The spectra of ^{40}Ar and ^{42}Ar contain information which can serve to determine the parameters c_{ik}. In ^{40}Ar a $K^\pi = 0^+$, $T = 2$ band is well established [18] starting with a 2121 keV level. The underlying Nilsson model configuration could either be $(1/2^-)^4(1/2^+)^2{}_{0,1}(3/2^-)^2{}_{0,1}$ or $(1/2^-)^4(1/2^+)^2{}_{0,1}(3/2^+)^2{}_{0,1}$. A large value of the intrinsic quadrupole moment $Q_0 = 1320^{+60}_{-120}$ mb speaks for the former configuration which contains altogether six particles in deformation-driving orbits (fig. 1). The head of a second band, based on the alternative configuration, has to be sought among two levels at 4420 and 4602 keV. They constitute the only states below 5.2 MeV excitation energy for which a $J^\pi = 0^+$ assignment is not excluded. One of these, I choose the 4420 keV state, is in fact available and not needed for completing the spectrum of spherical states with either a $(f\text{-}p)^2(s\text{-}d)^{-2}$ or $(f\text{-}p)^3(s\text{-}d)^{-3}$ shell-model configuration [4].

The ^{42}Ar level scheme below 3.1 MeV excitation energy is in one-to-one correspondence with shell-model predictions using the $(f\text{-}p)^4(s\text{-}d)^{-2}$ basis space [4] except for the 2512 keV, $J^\pi = 0^+$–4^+ state. This intruder is proposed here to constitute the head of a $K^\pi = 0^+$, $T = 3$ band based on the configuration $(1/2^-)^4(1/2^+)^2{}_{0,1}(3/2^-)^2{}_{0,1}(3/2^+)^2{}_{0,1}$. Values of the parameters c_{ik} as deduced from the spectra of ^{40}Ar and ^{42}Ar are given in table 2.

3.3 Assessment of parameters

The parameters of the Nilsson model phenomenology can be checked for plausibility. A state of the art Nilsson diagram for $A = 40$, obtained with use of a Woods-Saxon potential and extending to large values of the deformation parameters ε, has been given in [19]. It should differ

only marginally from the situation in $A = 37$ and underlies the schematic drawing of fig. 1. The theory places the $\Omega^\pi = 1/2^+, 3/2^-, 3/2^+$ single-particle orbits at relative energies of 0, 0.6 and 2.0 MeV in accordance with the neutron and proton binding energies of table 2, if a deformation parameter $\varepsilon = 0.37$ is chosen. The latter value comes close to the experimental [16] core deformation of 0.44 ± 0.03. The basic assumption of sect. 1 that the strongly deformation-driving $\Omega^\pi = 1/2^-$ orbit occurs below all other orbits of fig. 1 is confirmed and the experimentally inaccessible energy difference with respect to the $\Omega^\pi = 1/2^+$ orbit is given as -1.2 MeV. (The small value offers the possibility of a low-lying $K^\pi = 1/2^-$ band in ^{39}K with configuration $(1/2^-)^{-3}(1/2^+)^4$ which is outside the present model since it constitutes a core excitation. The $J^\pi = 3/2^-, 7/2^-, 1/2^-$ members of this strongly decoupled band can be identified with known levels at 4082, 4126, and 4475 keV excitation energy [1], while the $J^\pi = 15/2^-, 19/2^-, 23/2^-, 27/2^-$ members have possibly been observed [36] at 8008, 10264, 13009 and 16139 keV.) The slopes β_i of Nilsson orbits at core deformation needed in eqs. (8), (9) can equally be taken from fig. 1, and have values of 8, -6, and 11 MeV for $\Omega^\pi = 1/2^+$, $3/2^-$, and $3/2^+$, respectively.

The quartet binding energies of table 2 reflect the saturation properties of nuclear forces and values obtained in different mass regions should be comparable once the influence of nuclear sizes is removed. An analysis similar to the present one with use of an $A = 20$ rather than an $A = 36$ core [22] had yielded S_i values around -18 MeV. Values around -13.5 MeV can be expected in the present case (and are in fact observed) if the $A^{-1/2}$ mass dependence of pairing energies [37] is also adopted for the quartet energies.

The parameters a_{ik} and c_{ik} of table 2 degenerate in the spherical limit into the isoscalar and isovector monopole interaction energies a'_{ik} and c'_{ik} of the weak-coupling model. Standard values $a'_{ik} = -300$ keV, $c'_{ik} = -625$ keV used for the ^{40}Ca region [27] agree with corresponding results of table 2. To conclude, all parameters of the present model which can be checked for plausibility fulfil the criterion.

4 Experimental/theoretical binding energies and quadrupole deformations of bandheads between ^{36}Ar and ^{48}Cr

The empirical Nilsson model derived in the preceding section is used in table 3 to derive the energetically most favourable Nilsson model configurations of the $N \geq Z$ nuclei between ^{36}Ar and ^{48}Cr. The proton-rich mirror nuclei show essentially the same structure. The second and the third columns of table 3 give the occupancies of orbits and the quantum numbers of the resulting rotational bands. The orbits are ordered from left to right according to ascending single-particle energies as obtained in table 2. Subscripts to the occupancies $(2\Omega^\pi)^2$ indicate values of the intermediate quantum numbers K', T' which are cited, for the sake of simplicity, only if they deviate from the default values $K', T' = 0, 1$. The fourth column specifies the character of the Nilsson model configuration as a $n\hbar\omega$ excitation of the respective ground state with n being the difference of the added principal quantum numbers of all particles in, respectively, the deformed and the ground state. The quantity $n\hbar\omega$ is a measure of the excitation energy in the extreme independent-particle model. The fifth column gives a classification of the Nilsson model configuration by the number of particles with principal quantum number $N = 3$ and holes with $N = 2$. This classification remains valid if the wave functions of deformed states are expressed in terms of the spherical-shell model. The eighth column gives the theoretical binding energies of A-36 valence nucleons in the field of a deformed core as explained in sect. 2. (Note, however, a different treatment of the 6p-6h, $K^\pi = 0^+$ band of ^{40}Ca in appendix B.) Absence of an entry implies agreement with the experimental value since it was used in deriving the parameters of table 2. The experimental values of column seven represent the binding energies of the bandheads in column six, given relative to the 4329 keV, $J^\pi = 0^+$ state in ^{36}Ar and corrected in addition for the effect of zero point precession (sect. 2). The theoretical/experimental values of the deformation parameter have been obtained by the renormalized Racavy formula/from the $B(E2)$'s of inband transitions between the first few members of a band. Note, however, that use of $E2$ transitions between high-spin members is recommended in the case of the superdeformed 8p-8h band in ^{40}Ca [38].

The experimental data which were used for the evaluation of table 3 have been discussed to a considerable extent in the preceding section, already. The nuclides which have been treated and the relevant references are as follows:

^{36}Ar [16], ^{38}Ar [31,32], ^{40}Ar [18], ^{42}Ar [1], ^{38}K [1],
^{40}Ca [19], ^{41}Ca [1,39], ^{42}Ca [17,40], ^{42}Sc [1],
^{44}Ti [28,29], ^{48}Cr [30].

The mirror nuclei ^{37}Ar and ^{37}K, have been analyzed in table 1 and additional information on 6p-6h deformed states in ^{40}Ca and ^{40}K is given in appendix B. Rotational structure pertinent for the present work has also been observed in

^{43}Ca [41–43], ^{44}Ca [12,1], ^{43}Sc [13,14,44,45],
^{45}Sc [43], ^{46}V [35], and ^{47}V [45,46].

The heads of rotational bands in ^{39}Ar, ^{41}Ar, ^{39}K, ^{41}K and ^{43}K can be identified here because the levels in question do not find an explanation in shell-model calculations of $0\hbar\omega$ states or weak-coupling calculations of $1\hbar\omega$ states, while quantum numbers and excitation energies agree with the present predictions. Rotational structure in ^{42}K remains, however, unidentified because experimental deficiencies exist already with respect to the spherical part of the level spectrum.

In the case of ^{44}Sc the predicted $K^\pi = 0^-$ band is known [47], while the $K^\pi = 3^-$ band obtained by recoupling of the angular momentum projections still awaits identification. A $J = 3$ level at 531 keV excitation energy

Table 3. Nilsson orbit occupancies, bandhead excitation/binding energies and quadrupole deformation parameters ε of $A =$ 36–48 rotational bands.

Nuclide	Occupancies $(2\Omega^\pi)^n$ of Nilsson orbits[a]	K^π	Classification with respect to g.st.	Classification with respect to shell-closure	Bandhead energy [keV] E_x(exp.)[b]	E_B(exp)[c]	E_B(calc.)[c]	ε calc.	ε exp[d]
^{36}Ar	$(1^-)^4$	0^+	$4\hbar\omega$	4p-8h	4329	0		0.436	0.443
^{37}Ar	$(1^-)^4(1^+)^1$	$1/2^+$	$4\hbar\omega$	4p-7h	3980	−9176		0.407	
	$(1^-)^4\ (3^-)^1$	$3/2^-$	$5\hbar\omega$	5p-8h	4634	−8602		0.462	
^{38}Ar	$(1^-)^4(1^+)^2$	$0_1{}^+$	$4\hbar\omega$	4p-6h	3377	−21577		0.37	0.394
	$(1^-)^4\ (3^-)^2$	$0_2{}^+$	$6\hbar\omega$	6p-8h	4710	−20244	−19815	0.464	
^{39}Ar	$(1^-)^4(1^+)^2(3^-)^1$	$3/2^-$	$4\hbar\omega$	5p-6h	2433	−28458	−28277	0.385	
^{40}Ar	$(1^-)^4(1^+)^2(3^-)^2$	$0_1{}^+$	$4\hbar\omega$	6p-6h	2121	−39300		0.40	0.443
	$(1^-)^4(1^+)^2\ (3^+)^2$	$0_2{}^+$	$2\hbar\omega$	4p-4h	4420	−37011		0.31	
^{41}Ar	$(1^-)^4(1^+)^2(3^-)^2(3^+)^1$	$3/2^+$	$3\hbar\omega$	6p-5h	1035	−46606	−45613	0.371	
	$(1^-)^4(1^+)^2(3^-)^1(3^+)^2$	$3/2^-$	$2\hbar\omega$	5p-4h	1635	−46005	−44317	0.327	
	$(1^-)^4(1^+)^1(3^-)^2(3^+)^2$	$1/2^+$	$3\hbar\omega$	6p-5h	1869	−45691	−43603	0.371	
^{42}Ar	$(1^-)^4(1^+)^2(3^-)^2(3^+)^2$	0^+	$2\hbar\omega$	6p-4h	2512	−54432		0.343	
^{38}K	$(1^-)^4(1^+)^2{}_{1,0}$	1^+	$4\hbar\omega$	6p-4h	3978	−14361		0.37	
^{39}K	$(1^-)^4(1^+)^3$	$1/2^+$	$4\hbar\omega$	4p-5h	4095	−27280	−27556	0.338	
^{40}K	$(1^-)^4(1^+)^2(3^-)^2$	0^+	$5\hbar\omega$	6p-6h	1644	−37490		0.4	
^{41}K	$(1^-)^4(1^+)^3(3^-)^2$	$1/2^+$	$4\hbar\omega$	6p-5h	1593	−47677	−47121	0.37	
	$(1^-)^4(1^+)^2(3^-)^3$	$3/2^-$	$5\hbar\omega$	7p-6h	1582	−47768	−46640		
^{42}K	$(1^-)^4(1^+)^3(3^-)^2(3^+)^1$	1^+	$3\hbar\omega$	6p-4h			Average	0.34	
		2^+					−54538[e]		
	$(1^-)^4(1^+)^3(3^-)^1(3^+)^2$	1^-	$2\hbar\omega$	5p-3h			Average[f]	0.30	
		2^-					−53453		
^{43}K	$(1^-)^4(1^+)^3(3^-)^2(3^+)^2$	$1/2^+$	$2\hbar\omega$	6p-3h	(1866)	−64579	−64277	0.316	
	$(1^-)^4(1^+)^2(3^-)^2(3^+)^3$	$3/2^+$	$2\hbar\omega$	6p-3h	1110	−65415	−64462	0.316	
^{40}Ca	$(1^-)^4(1^+)^4$	$0_1{}^+$	$4\hbar\omega$	4p-4h	3353	−36311		0.31	0.264
	$(1^-)^4\ (3^-)^4$	$0_2{}^+$	$8\hbar\omega$	8p-8h	5212	−34453	−33096	0.487	0.569
	$(1^-)^4(1^+)^2(3^-)^2$	$0_3{}^+$		6p-6h	7702	−31962	−32605[g]	0.4	
	$(1^-)^4\ (3^+)^4$	$0_4{}^+$	$4\hbar\omega$	4p-4h	7815	−31849		0.31	
^{41}Ca	$(1^-)^4(1^+)^4(3^-)^1$	$3/2^-$	$4\hbar\omega$	5p-4h	2462	−45685		0.308	0.248
	$(1^-)^4(1^+)^4\ (3^+)^1$	$3/2^+$	$3\hbar\omega$	4p-3h	3050	−45098			
	$(1^-)^4(1^+)^1(3^-)^4$	$1/2^+$	$7\hbar\omega$	8p-7h	3845	−44222	−43044	0.456	
^{42}Ca	$(1^-)^4(1^+)^4(3^-)^2$	$0_1{}^+$	$4\hbar\omega$	6p-4h	1837	−57670		0.34	0.395
	$(1^-)^4(1^+)^4\ (3^+)^2$	$0_2{}^+$	$2\hbar\omega$	4p-2h	3300	−56207		0.256	
^{43}Ca	$(1^-)^4(1^+)^4(3^-)^2(3^+)^1$	$3/2^+$	$3\hbar\omega$	6p-3h	990	−66450	−66286	0.314	0.315
	$(1^-)^4(1^+)^4(3^-)^1(3^+)^2$	$3/2^-$	$2\hbar\omega$	5p-2h	2102	−65338	−65409	0.274	0.315
^{44}Ca	$(1^-)^4(1^+)^4(3^-)^2(3^+)^2$	0^+	$2\hbar\omega$	2p-2h	1883	−76688	−77224	0.29	
^{42}Sc	$(1^-)^4(1^+)^4(3^-)^2{}_{3,0}$	$3_1{}^+$	$4\hbar\omega$	6p-4h	2223	−50319		0.34	
	$(1^-)^4(1^+)^4\ (3^+)^2{}_{3,0}$	$3_2{}^+$	$2\hbar\omega$	4p-2h	1846	−50696		0.256	

and a 1006 keV, $J^\pi = 3, 4^-$ level are available and could constitute the first members of the band. The spectrum of positive-parity states in ^{44}Sc below 1.2 MeV excitation energy yields a surplus of just a single $J^\pi = 3^+$ state over the predictions of a shell-model calculation in a $(f\text{-}p)^4$ basis space. One out of the 763, 987 and 1186 keV, $J^\pi = 3^+$ levels has intruder status and could constitute the head of the predicted $K^\pi = 3^+$ band of table 3. A retarded γ-decay seems to exclude an $(f\text{-}p)^4$ character of the 987 keV level.

5 Assessment of results

The theory of deformed intrinsic states in $A = 36$–48 nuclei as developed in the preceding sections is successful in reproducing both binding energies and quadrupole deformations. Table 3 contains a sample of 58 experimental binding energies. While 20 of these were used to fix the parameters of the nuclear interactions another 38 are predicted with 2% accuracy. Significance of results is thus established. Particularly gratifying is the good reproduction of binding energies for the $K^\pi = 0^+$ configurations of ^{48}Cr and ^{44}Ca. The nuclide ^{48}Cr is fairly remote, already, from the $A = 36$–44 mass region where the parameters of the theory were fixed while ^{44}Ca exhibits the largest neutron excess of all nuclides which were not used in the fitting procedure. Equally gratifying is the reproduction of the superdeformed $K^\pi = 0_2{}^+$ configuration in ^{40}Ca since it constitutes a $8\hbar\omega$ excitation of the respective ground state with an extremely small bandhead excitation energy

Table 3. Continued.

Nuclide	Occupancies $(2\Omega^\pi)^n$ of Nilsson orbits[a]	K^π	Classification with respect to g.st.	Classification with respect to shell-closure	Bandhead energy [keV] E_x(exp.)[b]	E_B(exp)[c]	E_B(calc.)[c]	ε calc.	ε exp[d]
^{43}Sc	$(1^-)^4(1^+)^4(3^-)^3$	$3/2^-$	$4\hbar\omega$	7p-4h	472	−64085		0.358	0.305
	$(1^-)^4(1^+)^4\quad(3^+)^3$	$3/2^+$	$1\hbar\omega$	4p-1h	151	−64406	−63867	0.232	0.261
	$(1^-)^4(1^+)^3(3^-)^4$	$1/2^+$	$5\hbar\omega$	8p-5h	855	−64548	−63452	0.398	0.366
^{44}Sc	$(1^-)^4(1^+)^4(3^-)^1(3^+)^3$	$0^-(J=\text{even})$	$1\hbar\omega$	5p-1h	146	Average	Average		
		$(J=\text{odd})$			68	−74003	−73537	0.25	0.232
	$(1^-)^4(1^+)^4(3^-)^1(3^+)^3$	3^-			531				
	$(1^-)^4(1^+)^4(3^-)^2(3^+)^2{}_{3,0}$	3^+	$2\hbar\omega$	6p-2h	(987)	−73388	−73104	0.29	
^{45}Sc	$(1^-)^4(1^+)^4(3^-)^2(3^+)^3$	$3/2^+$	$1\hbar\omega$	6p-1h	12	−85652	−85923	0.267	0.252
	$(1^-)^4(1^+)^3(3^-)^2(3^+)^4$	$1/2^+$	$1\hbar\omega$	6p-1h	939	−84555	−85745	0.267	
^{44}Ti	$(1^-)^4(1^+)^4\quad(3^+)^4$	$0_1{}^+$	$0\hbar\omega$	4p	0	−73087		0.21	0.224
	$(1^-)^4(1^+)^4(3^-)^4$	$0_2{}^+$	$4\hbar\omega$	8p-4h	1904	−71183		0.372	0.282
	$(1^-)^4\quad(3^-)^4(3^+)^4$	$0_3{}^+$	$4\hbar\omega$	8p-4h	4840	−68247		0.372	
^{45}Ti	$(1^-)^4(1^+)^4(3^-)^4(3^+)^1$	$3/2^+$	$3\hbar\omega$	8p-3h	329	−82401	−81026	0.346	0.332
	$(1^-)^4(1^+)^3(3^-)^4(3^+)^4$	$1/2^+$	$3\hbar\omega$	8p-3h	1565	−81245	−79520	0.346	
^{46}Ti	$(1^-)^4(1^+)^4(3^-)^4(3^+)^2$	$0_2{}^+$	$2\hbar\omega$	8p-2h	≥ 2611	≤ -93014	−93174	0.32	
	$(1^-)^4(1^+)^4(3^-)^2{}_{0,0}(3^+)^4$	$0_1{}^+$	$0\hbar\omega$	6p	0	−95726	−96554	0.25	
^{46}V	$(1^-)^4(1^+)^4(3^-)^2(3^+)^4$	0^+	$0\hbar\omega$	6p	993	−87135	−88604	0.25	
	$(1^-)^4(1^+)^4(3^-)^2{}_{3,0}(3^+)^4$	3^+	$0\hbar\omega$	6p	801	−87409	−88483	0.25	0.212
	$(1^-)^4(1^+)^4(3^-)^3(3^+)^3$	$0^-(J=\text{even})$	$1\hbar\omega$	7p-1h	1235	Average	Average		
		$(J=\text{odd})$			~ 1200[h]	−86893	−85208	0.284	0.266
	$(1^-)^4(1^+)^4(3^-)^3(3^+)^3$	3^-			1254				
^{47}V	$(1^-)^4(1^+)^4(3^-)^4(3^+)^3$	$3/2^+$	$1\hbar\omega$	8p-1h	260	−100834	−101190	0.299	0.366
	$(1^-)^4(1^+)^4(3^-)^3(3^+)^4$	$3/2^-$	$0\hbar\omega$	7p	0	−101093	−102552	0.26	0.234
	$(1^-)^4(1^+)^3(3^-)^4(3^+)^4$	$1/2^+$	$1\hbar\omega$	8p-1h	1660	−99354	−100992	0.299	0.304
^{48}Cr	$(1^-)^4(1^+)^4(3^-)^4(3^+)^4$	0^+	$0\hbar\omega$	8p	0	−109074	−110739	0.26	0.283

([a]) The complete specification of orbits is given in fig. 1. Intermediate quantum number K', T' of particle pairs are given as subscripts, if they deviate from the default values $0, 1$.

The isospin of configurations is $T = (N - Z)/2$.

([b]) See text.

([c]) Binding energies calculated relative to the 4329 keV level of ^{36}Ar after having removed the energy of zero-point precession.

([d]) From $B(E2)$'s of inband transitions. For references see text.

([e]) Corresponding to $E_x = 2436$ keV.

([f]) Corresponding to $E_x = 3431$ keV.

([g]) Calculated with the alternative method of appendix B. See footnotes to table 2 in addition.

([h]) Extrapolated bandhead energy obtained with use of the $J(J+1)$ rule of excitatoin energies.

of 5212 keV only. The theoretical value of 6570 keV comes very close and it will improve further to something like 6 MeV by virtue of configuration mixing. This effect (not contained in the present theory) is not negligible as shown by a very recent investigation of inband $B(E2)$'s [38]. The mixing is due to the presence of the nearby 6p-6h intrinsic state of equal K^π in table 3 which was postulated already in the work of Gerace and Green [10]. The postulate has a firm basis now which is discussed in appendix B. The low-lying 8p-8h state must inevitably be the parent of a low-lying 8p-7h, $K^\pi = 1/2^+$ band in ^{41}Ca. Good experimental-theoretical agreement of binding energies is in fact achieved (table 3) by identifying the 3845 keV level of fig. 2 with the bandhead.

The occupation of orbits in the isotopes of Ar, K and Ca is governed by the single-particle energies of table 2, so that the $\Omega^\pi = 3/2^-$ orbits gets occupied prior to the $\Omega^\pi = 3/2^+$ orbit. The situation changes when the sphericity-driving $\Omega^\pi = 1/2^+$ and $\Omega^\pi = 3/2^+$ orbits contain, together, seven or eight nucleons. The energy gain by rearrangement of the nuclear shape (eq. (9)) which is implicit in the theory can dominate the single-particle energies and lead to the occupation of the $\Omega^\pi = 3/2^+$ orbit prior to the $\Omega^\pi = 3/2^-$ orbit. This situation can and in fact does occur in the isotopes of Sc, Ti, and V.

The competition of orbits leads to several new assignments of configurations to rotational bands compared to previous work. The new assignments have in common that two more particles reside in orbits with principal quantum number $N = 3$ than was previously believed or, in other words, an $n\hbar\omega$ excitation is replaced by a $(n+2)\hbar\omega$ excitation. Such changes have happened for the $K^\pi = 0_1{}^+$ band of ^{42}Ca [11], the $K^\pi = 3/2^+$, $1/2^+$ and $3/2^-$ bands of ^{43}Sc [13,14], the $K^\pi = 3/2^+$ band of ^{45}Ti [44] and the $K^\pi = 0_1{}^+$ band of ^{40}Ar [18], which was tacitly believed to constitute a 4p-4h rather than a 6p-6h configuration. Quite generally we have a tendency towards multi-particle excitations from $N = 2$ into $N = 3$ orbits. Table 3 contains

sixteen $4\hbar\omega$ excitations of the respective ground state and seven $(5-8)\hbar\omega$ excitations.

The assignments of configurations to bands finds its most convincing support in the experimental-theoretical agreement of quadrupole deformations in table 3. The renormalized Racavy expression reproduces the experimental values within the error limits. The renormalization factor adopted from an analysis in the lower *s-d* shell seems to have a wider range of applicability. Values of the deformation parameter ε vary between a high one of 0.56 ± 0.09 in ^{40}Ca to a low one of 0.22 ± 0.04 in ^{44}Ti. The theory follows these variations very faithfully even though Racavy's formula is valid, strictly speaking, in the limits of large deformations only, where the problem of double-counting of interactions [21] is avoided. Evidently perturbations at smaller deformations (says $\varepsilon < 0.3$) are not important yet compared to uncertainties of the experimental values. Thus, it is possible to quantify the frequently used arguments of deformation or sphericity-driving orbits and to make reliable predictions of deformations where experimental data are not available.

To conclude, a reliable accounting is achieved of rotational bands in the $A = 36$–48 mass region which are based on axially symmetric intrinsic states. The next section will deal with possible deviations from axial symmetry.

6 Gamma-vibrational and rotation-aligned bands

Deviations from axial symmetry can be inferred for several deformed intrinsic states of the ^{40}Ca region and be related to two mechanisms. Excitation of the γ-vibration is an issue since the days of Gerace and Green [10]. It leads to the presence of additional $K^\pi = 2^+$ bands in even-even nuclei and of $K = (\Omega \pm 2)$ bands in odd-A nuclei. Rotation alignment of a particle pair, well known in heavier nuclei, is a new facet for the ^{40}Ca region and is discussed here for the first time. I begin with mounting evidence in favour of γ-vibrational bands.

The presence of a $K^\pi = 2^+$ band in ^{44}Ti based on the 2530 keV, 2^+ state has been established long time ago [28]. In the case of ^{40}Ca members of a first $K^\pi = 2^+$ band based on the 5249 keV, 2^+ state (fig. 3) have been traced recently up to the $J^\pi = 15^+$ member at 19197 keV [19]. A staggering of excitation energies according to even or odd spin is indicative of a strong rotation-vibration interaction with the first $K^\pi = 0^+$ band, which constitutes the parent.

The present work gives the first evidence of γ-vibrational bands in the odd-A nucleus ^{41}Ca and in doubly-odd ^{42}Sc. In the case of ^{41}Ca two normal bands with quantum numbers $K^\pi = 3/2^-$ and $K^\pi = 3/2^+$ seem to be accompanied (fig. 2) by a pair of bands, each, with respectively $K^\pi = 7/2^-$, $1/2^-$ and $K^\pi = 7/2^+$, $1/2^+$. In the case of ^{42}Sc the analysis of fig. 4 has revealed the presence of a low-lying $K^\pi = 1^+$ band based on the 1889 keV state. This band is difficult to obtain with the construction principles of sect. 2 and an interpretation as a γ-vibrational band, derived from the lowest-lying, $K^\pi = 3_1^+$ band of fig. 4, is thus appealing. The remarkably low excitation energy of the $K^\pi = 1^+$ band can in fact be tied to the equally low excitation energy of the $K^\pi = 2^+$ γ-vibrational band in ^{40}Ca. The leading configuration of the latter band is, within a microscopic description, inevitably $(1/2^-)^4((1/2^+)^3(3/2^+)^1)_{2,0}$ while the leading configuration of the ^{42}Sc band had already been given in subsect. 3.2.2 as $(1/2^-)^4((1/2^+)^3(3/2^+)^3)_{1,0}$. Both configurations behave equally with respect to the energy gain by the two isospin-dependent terms of eq. (5). This gain, which is calculable here only in part, is decisive and of the order -4 MeV. Hence, if the ^{40}Ca bands gets depressed so does the ^{42}Sc band. Another consequence of the microscopic structure which underlies the ^{40}Ca band is the prediction of a second $K^\pi = 2^+$, $T = 0$ band at a distance of 2 MeV with configuration $(1/2^-)^4((1/2^+)^1(3/2^+)^3)_{2,0}$. The experimental data in fig. 3 seems to reflect exactly this situation. The $J^\pi = 2^+$, 3^+, 4^+ levels at $E_x = 6909$, 7561 and 8374 keV are available and occur at the proper energies as it is the case for the $J^\pi = 13^+$ and 14^+ states [19] at 16581 and 17700 keV.

A new facet of rotational structure for the ^{40}Ca region seems to emerge from a recent observation [19] of yrast states with $E_x(J^\pi) = 8103$ keV (8^+), 11005 keV (10^+), 13117 keV (12^+), and 16531 keV (14^+), which have not found an explanation yet. The concept of rotation-aligned bands offers a solution. The first $K^\pi = 0^+$ band, based on the 3353 keV level has an underlying configuration with two pairs of like particles in the $\Omega^\pi = 1/2^-$ orbit of fig. 1 which is derived from a shell-model orbit of large j (the $f_{7/2}$ orbit). If, under the influence of the Corriolis force, a pair of like particles aligns its angular momentum along the axis of collective rotation, a series of levels with, in order of ascending energies, $J^\pi = 6^+$, 8^+, $10^+ \ldots$ will arise. The 7677 keV, $J^\pi = 6^+$ level of ^{40}Ca, equally without interpretation yet, could be the lowest-lying member of the rotation-aligned band.

7 Summary

The model of coexisting spherical and deformed states has been applied to the doubly-magic nucleus ^{40}Ca [9,10] and its neighbours [11–14] some thirty years ago in an attempt to explain the high level densities of these nuclei. One generation later we are able to fully asses its range of validity. The spherical states are well under control now due to the general progress of spectroscopy [1] and the development of shell-model calculations [3–8] which allow cross-checks for completeness of the experimental information. By the same token it is possible to locate levels of different character by the principle of exclusion. The experimental investigation of deformed states has entered a new stage due to the availability of large detector arrays for γ-radiation and has resulted in the recent observation of superdeformation in ^{40}Ca [19] and ^{36}Ar [16]. The ^{36}Ar result suggests that low-lying deformed states are a general feature of nuclei between ^{36}Ar and ^{48}Cr. Starting from the deformed intrinsic state of ^{36}Ar as a core, it has been possible in this work to construct a Nilsson model which, in analogy to

the spherical case, uses empirical single-particle energies and residual interactions. The derivation of single-particle energies from the spectra of $A = 37$, $T = 1/2$ is of key importance in this respect and was possible only, because existence of bandheads could be traced in a dense spectrum of surrounding spherical states. The phenomenological Nilsson model is successful in predicting and reproducing the deformed states of lowest energy in all nuclei of the considered mass region. The empirical approach allows to incorporate the rearrangement energies which arise, if the addition of valence nucleons to the core results in a new equilibrium deformation. Compared to previous work larger deformations are considered with the consequence that more particles than previously believed [11–14] are found in orbits which are derived from the $f_{7/2}$ shell-model state. Expressed differently, it is necessary to incorporate $n\hbar\omega$ excitations of higher n.

The systematics of deformed, axially symmetric states, if amended by a few deviations from axial symmetry due to γ-vibrations or rotation alignment, is hundred percent complementary to the spherical states. In other words, all the degrees of freedom have in fact been located, which govern the structure of nuclei in the transitional region from the *s-d* into the *f-p* shell.

Between ^{36}Ar and ^{43}Sc we observe a clear distinction between a spherical and deformed minimum of the total energy. The distinction gets lost on the way from ^{44}Ti to ^{48}Cr. Both minima start moving towards an intermediate value of the deformation parameter and equally the energetical difference levels off. The nuclides ^{46}Ti, ^{46}V, ^{47}V, and ^{48}Cr are moderately deformed in their ground states. The resulting rotational bands are described by shell-model calculations [4–7] which invoke either no excitations of particles from the $N = 2$ into the $N = 3$ major shell, or a single excitation only. From the point of view of the Nilsson model, however, all nuclides between ^{36}Ar and ^{48}Cr can be treated on an equal footing.

Appendix A. Coulomb interactions

The Coulomb interaction energies of deformed states are subdivided in sect. 2 into contributions E_i and e_{ik} of two protons in, respectively, identical or different Nilsson orbits. They can be deduced from the binding energies of mirror analogue states [1].

The values of E_i are best obtained by using configurations with three nucleons in a single orbit as they occur in $A = 4n + 3$ nuclei. Binding energies of mirror analogue states differ in just one unit of E_i and in the single-particle energies of protons and neutrons which in turn follow from single-particle configurations in $A = 4n+1$ nuclei. The values of E_i in table 2 from top to bottom are thus given by the expressions

$$^{39}\mathrm{Ca}(4012) - {}^{39}\mathrm{K}(4095) - {}^{37}\mathrm{K}(3840) + {}^{37}\mathrm{Ar}(3980),$$
$$^{43}\mathrm{Ti}(475) - {}^{43}\mathrm{Sc}(472) - {}^{41}\mathrm{Sc}(2424) + {}^{41}\mathrm{Ca}(2462),$$
$$^{43}\mathrm{Ti}(313) - {}^{43}\mathrm{Sc}(151) - {}^{41}\mathrm{Sc}(3013) + {}^{41}\mathrm{Ca}(3049),$$

where the symbols of the nuclides stand for the atomic mass excesses [48] of the specified excited state.

The interaction energies e_{ik} are obtained by considering the interaction energies of both a single proton and a single neutron in orbit i with two cores, which differ by just the completely filled orbit k. The same method can be applied to single-hole states. The values of e_{ik} in table 2 from top to bottom are given by the expressions

$$0.5\big(^{47}\mathrm{Cr}(1831) - {}^{43}\mathrm{Ti}(1022) - {}^{47}\mathrm{V}(1660) + {}^{43}\mathrm{Sc}(855)\big),$$
$$0.5\big(^{41}\mathrm{Sc}(2414) - {}^{41}\mathrm{Ca}(2462) - {}^{37}\mathrm{K}(4278) + {}^{37}\mathrm{Ar}(4634)\big),$$
$$0.5\big(^{45}\mathrm{V}(385) - {}^{45}\mathrm{Ti}(329) - {}^{41}\mathrm{Sc}(3013) + {}^{41}\mathrm{Ca}(3049)\big).$$

The Nilsson model configurations of the specified levels can be read from table 3 in the case of neutron-rich nuclei and equally be assigned to their mirror analogues.

Appendix B. 2p-2h and 6p-6h states in A = 40

The $A = 40$ system contains deformed $K^\pi = 0^+$, 6p-6h states (table 3) with $T_\mathrm{p} = T_\mathrm{h} = 1$, $T = 0, 1$ or 2. They compete in energy with, and must be distinguished from, spherical 2p-2h states of equal isospin structure. The present appendix deals with the identification of the lowest-lying $J^\pi = 0^+$ states of both configurations. While the $T = 2$ levels are well known, difficulties exist with respect to the $T = 1$ states. Once they are removed, it will be possible to deduce the isospin-splitting term of the residual interaction with improved accuracy as compared to the results of table 2 or, in the case of 2p-2h states, standard [27] weak-coupling calculations. This leads to a safer prediction and subsequent identification of the $T = 0$ states because the isospin splitting between the $T = 2$ and $T = 1$ levels is just twice as large as the splitting between the $T = 1$ and $T = 0$ states.

Levels with $T = 2$ character are best studied in ^{40}Ar where they provide the spectrum of low-lying states. The ground and 2121 keV, $J^\pi = 0^+$ states constitute the 2p-2h [4] and, respectively, 6p-6h [18] excitations as discussed in subsect. 3.2.3. Their ^{40}Ca analogues, needed below, occur [1] or are expected at 11988 keV and, respectively, 14.1 ± 0.1 MeV excitation energy. The $T = 1$ spectrum contains a single $J^\pi = 0^+$ state only which occurs at 1644 keV excitation energy in ^{40}K and 9408 keV in ^{40}Ca [1]. Both detailed shell-model calculations [4] and the transparent weak-coupling model [27] exclude a 2p-2h character because the expected excitation energy is significantly lower, being 717 keV in shell-model calculations for ^{40}K. The alternative assignment of a 6p-6h character will gain additional credibility if the missing 2p-2h state gets identified. The apparent absence of this level in all of the nuclides ^{40}Sc, ^{40}Ca, and ^{40}K turns out to be the result of a circle conclusion starting from the apparent absence in the ^{40}K spectrum.

The missing $J^\pi = 0^+$ state of ^{40}K should have been observed in the clean particle spectrum of the ^{39}K(d, p) reaction [49] unless it coincides to within a few keV with the second or third excited state at, respectively, 800 or

891 keV excitation energy. The mirror nuclide ^{40}Sc has been investigated with the ^{40}Ca(τ, t) reaction [50]. An unassigned peak is clearly visible in the published particle spectrum which could correspond to a ^{40}Sc level at 808 keV excitation energy. It remained unattended because of the seeming absence of a mirror analogue in ^{40}K. The ^{40}Ca spectrum (fig. 3) contains a $J^\pi = 0^+$ level of unknown isospin at an excitation energy of 8439 keV, 781 keV above the first $T = 1$ state. A $T = 1$ assignment of this level was, once more, not considered because of the missing ^{40}K state. A 8.28 ± 0.1 MeV state of ^{40}Ca is reached in the ^{38}Ar(τ, n) reaction [51] by $L = 0$ transfer with a large cross-section. In view of the 400 keV energy resolution it is feasible that the 8439 keV level has been observed which would then support a 2p-2h character. It appears that the first $J^\pi = 0^+$, $T = 1$ state of the $A = 40$ system has been missed by unfortunate circumstances and that its excitation energy above the first $T = 1$ state is given as 808 keV in ^{40}Sc, 781 keV in ^{40}Ca, and 800 keV in ^{40}K. The shell-model prediction for ^{40}K is 717 keV with an uncertainty of roughly 300 keV. To say the least, one cannot turn the argument of a missing 2p-2h state against a 6p-6h assignment to the established $J^\pi = 0^+$ level at 1644 keV in ^{40}K and, respectively, 9408 keV in ^{40}Ca.

After having established the 6p-6h states of $T = 2$ and $T = 1$ character at, respectively, 14.1 MeV and 9408 keV excitation energy in ^{40}Ca it is possible to predict the corresponding $T = 0$ state at 7059 keV. Similarly, strong arguments speak for a 2p-2h state at 6664 keV. These energies will increase by up to 1 MeV due to configuration mixing. The effect has been investigated in the early work of Gerace and Green [10] who anticipated low-lying 6p-6h and 2p-2h states in order to establish a coupling mechanism between the 0p-0h, 4p-4h and 8p-8h configurations. Their unperturbed 6p-6h and 2p-2h energies coincide with the present results to within 0.5 MeV and hence their conclusions with respect to configuration mixing can be adopted here.

It is straightforward to assign 2p-2h character to the experimental $0_4{}^+$ state at 7301 keV excitation energy since no other state is available below 7.7 MeV. Contrary to this situation four levels (at 7702, 7815, 8019 and 8276 keV) exist which could correspond to the predicted 6p-6h state. The ^{42}Ca(p, t) pick-up reaction [52] selects the 7702 keV, $0_5{}^+$ state. The ^{42}Ca ground state is known to mix with the deformed first excited $J^\pi = 0^+$ state [53] which, as shown in table 3, has a 6p-4h (rather than a 4p-2h) character. Due to this admixture $L = 0$ pick-up of two $f_{7/2}$ particles (rather than $d_{3/2}$ particles) is leading to the 4p-4h, $J^\pi = 0^+$ of ^{40}Ca at 3353 keV excitation energy. Pick-up of two $d_{3/2}$ particles leads to the 6p-6h, $J^\pi = 0^+$ state. Experiment shows the expected strong excitation of the 3353 keV state, and of the 7702 keV, $0_5{}^+$ state as well.

At the end of the analysis we have arrived at exactly the Gerace and Green interpretation [10] of the first five $J^\pi = 0^+$, $T = 0$ levels in ^{40}Ca which was called "little more than a conjecture" by the authors. To be added is the interpretation (subsect. 3.2.1) of the 7815 keV, $0_6{}^+$ level as the second 4p-4h, $K^\pi = 0^+$ state.

Appendix C. Negative-parity, T = 0 states in ^{40}Ca

The methods developed in this paper shed light on the structure of the negative-parity, $T = 0$ states in ^{40}Ca which are not as well known as are the positive-parity ones. Gerace and Green [54] have proposed coexistence of spherical 1p-1h states with deformed 3p-3h states, which constitute a $K^\pi = 1^-$ rotational band. Today's improved knowledge of the level scheme and the new insight into the generation of deformed states require a major revision in the sense that the lowest-lying 3p-3h states maintain a spherical character while deformed 5p-5h and 7p-7h states have to be added (fig. 3).

The alleged 3p-3h, deformed intrinsic state of Gerace and Green is based, in the notation of this work, on the Nilsson model configuration $(1/2^-)^3(1/2^+)^4(3/2^+)^1$. The associated value of the deformation parameter, calculated with the methods of this work, is $\varepsilon = 0.25$ only and it is feasible that a rotational sequence of levels does not develop. The lowest-lying 3p-3h states could alternatively be members of the $J^\pi = 2^-$–5^- weak-coupling multiplet, which is due to the coupling of an odd $f_{7/2}$ particle with an odd $d_{3/2}$ hole. Two more groups with $J^\pi = 0^-$–3^- and 3^-, 4^- are expected at a distance of about 1.2 MeV. In other words the 3p-3h spectrum reflects the structure of the 1p-1h spectrum of fig. 3 with a somewhat smaller spacing of multiplets. The observable consequence of sphericity is thus a proliferation of negative-parity levels with relatively high spin of $J = 4$ or 5. The apparently well-established $K^\pi = 1^-$ band of [54] must find another explanation. The theoretical framework of the present paper allows to predict two $K^\pi = 1^-$ and 2^- pairs of rotational bands based on the 5p-5h configuration $(1/2^-)^4(1/2^+)^3(3/2^-)^1$ and, respectively, the 7p-7h configuration $(1/2^-)^4(1/2^+)^1(3/2^-)^3$. The bandhead energies for $K^\pi = 1^-$ and 2^- cannot be predicted separately because the coefficients b_{ik} and d_{ik} of eq. (5) are unknown but the mean value comes out as 8.3 MeV in the former case and as 10.1 MeV in the latter one. In addition both the $K^\pi = 2^-$ bands and the $K^\pi = 1^-$ bands are separated by the same amount of 1.8 MeV as are the mean values.

In order to check the new interpretation, it becomes necessary to complete parity assignments to the $T = 0$ levels in ^{40}Ca up to 8 MeV in excitation. The γ-decay modes of these states are known in some detail [1] and can serve for this purpose because of the strong retardation [45], not to say forbiddances, of $E1$ decay between $T = 0$ states. Thus, it is highly unlikely that a positive-parity state will decay exclusively to final states of negative parity because the retardation of such $E1$ decays would not be counteracted by a more favourable transition energy as compared to parity conserving transitions (fig. 3). With this argument negative parity can be assigned to levels at 7928, 7769, 7239, 7422 and 7278 keV excitation energy superseding previous assignments to the 7928 and 7278 keV levels from angular distributions of inelastically scattered protons [55]. The first three of these decay to the $J^\pi = 4_1{}^-$ or $5_1{}^-$ levels of fig. 3 and are thus candidates for a $J^\pi = 4^-$ or

5^- assignment, leaving $J^\pi = 3^-$ as a less likely alternative. It seems feasible in addition to exclude the $J^\pi = 5^-$ alternative for the 7928 keV level because this state is probably fed from a $J^\pi = 3^+$, $T = 1$ resonance of the ^{39}K(p,γ) reaction [56]. Three levels at $E_x = 7623$, 7446 and 6931 keV decay to final states of either parity and remain without a parity assignment henceforth, however their spin is delimited to $J = 3$ under the assumption of negative parity. While there is a clear demand from the theoretical side for additional $J^\pi = 3^-$ states it would be difficult to accommodate additional levels in the already very complete spectrum of positive-parity states in fig. 3. By adopting the $J^\pi = 3^-$ assignments, it is possible to construct a spectrum of negative-parity, $T = 0$ states in agreement with the proposals made in this appendix. Figure 3 contains in first place all the 1p-1h states which can be reasonably expected [4] below 8 MeV excitation energy. The $K^\pi = 1_1{}^-$ band proposed long time ago can be extended now to include the unique $J^\pi = 5^-$ candidate at 7769 keV from the present work and possibly the 8851 keV state from inelastic proton scattering as the $J^\pi = 6^-$ member [55]. Room is left for a rotational sequence of levels on top of the 1_3^-, 7113 keV state and for a $K^\pi = 2^-$ band which is expected to accompany the first $K^\pi = 1^-$ band. The remaining states, especially the prospective $J^\pi = 4^-$ state at 7928 keV and the $J^\pi = 4^-, 5^-$ candidate at 7239 keV are accounted for by the first 3p-3h multiplets of spherical character with $J^\pi = 2^-$–5^-, 0^-–3^- and 3^-, 4^-. The mean of the $K^\pi = 1_1{}^-$ and 2^- bandhead energies is 6.59 MeV in good agreement with a value of 8.3 MeV predicted for the 5p-5h, deformed configuration. The difference in energy between the $K^\pi = 1_2{}^-$ and $1_1{}^-$ bands amounts to 1.2 MeV in good agreement with the predicted difference of 1.8 MeV between the 7p-7h and 5p-5h bands of equal K^π.

In conclusion, we seem to have observed all np-nh, $T = 0$ excitations with $n = 1$–8 which in turn account for the complete spectrum of excited states in ^{40}Ca below 8 MeV excitation energy. Spherical character is indicated for $n = 1$–3 and deformed character for $n = 4$–8.

References

1. P.M. Endt, Nucl. Phys. A **521**, 1 (1990); **633**, 1 (1998).
2. A.M. Bernstein, Ann. Phys. (N.Y.) **69**, 19 (1972).
3. B.H. Wildenthal, in *Progress in Particle and Nuclear Physics*, edited by D.H. Wilkinson (Plenum Press, New York, 1984).
4. E.K. Warburton, J.A. Becker, D.J. Millener, B.A. Brown, Brookhaven National Laboratory Report, 40890 (1987) unpublished.
5. E. Caurier, A.P. Zucker, A. Poves, G. Martinez-Pinedo, Phys. Rev. C **50**, 225 (1994).
6. G. Martinez-Pinedo, A.P. Zucker, A. Poves, E. Caurier, Phys. Rev. C **55**, 187 (1997).
7. A. Poves, J. Sanchez-Solano, Phys. Rev. C **58**, 179 (1998).
8. S.M. Lenzi *et al.*, Phys. Rev. C **60**, 021303 (R) (1999).
9. W.J. Gerace, A.M. Green, Nucl. Phys. A **93**, 110 (1967).
10. W.J. Gerace, A.M. Greene, Nucl. Phys. A **123**, 241 (1969).
11. B.H. Flowers, L.D. Skouras, Nucl. Phys. A **136**, 353 (1969).
12. L.D. Skouras, Nucl. Phys. A **220**, 604 (1974).
13. I.P. Johnstone, Nucl. Phys. A **110**, 429 (1968).
14. I.P. Johnstone, G.L. Payne, Nucl. Phys. A **124**, 217 (1969).
15. D.M. Brink, A.K. Kerman, Nucl. Phys. **12**, 314 (1959).
16. C.E. Svensson *et al.*, Phys. Rev. C **63**, 061301-1 (2001).
17. P. Betz, E. Bitterwolf, B. Busshardt, H. Röpke, Z. Phys. A **276**, 295 (1976).
18. E. Bitterwolf *et al.*, Z. Phys. A **313**, 123 (1983).
19. E. Ideguchi *et al.*, Phys. Rev. Lett. **87**, 222501-1 (2001).
20. G. Rakavy, Nucl. Phys. **4**, 375 (1957).
21. S.G. Nilsson, Mat.-Fys. Medd. K. Dan. Vidensk. Selsk. **29**, no. 16 (1955).
22. H. Röpke, Nucl. Phys. A **674**, 95 (2000).
23. M. Carchichi, B.H. Wildenthal, Phys. Rev. C **37**, 1681 (1988).
24. P.J. Nolan *et al.*, J. Phys. G **1**, 35 (1975).
25. H. Hasper, Phys. Rev. C **19**, 1482 (1979).
26. B.A. Brown, B.H. Wildenthal, At. Data Nucl. Data Tables **33**, 347 (1985).
27. J.J. Kolata, J.W. Olness, E.K. Warburton, A.R. Poletti, Phys. Rev. C **13**, 1944 (1976).
28. W.W. Simpson, W.R. Dixon, R.S. Storey, Phys. Rev. Lett. **31**, 946 (1973).
29. C.D. O'Leary *et al.*, Phys. Rev. C **61**, 064314 (2000).
30. F. Brandolini *et al.*, Nucl. Phys. A **642**, 387 (1998).
31. P. Betz, H. Röpke, F. Glatz, G. Hammel, V. Glattes, W. Brendler, Z. Phys. **271**, 195 (1974).
32. D. Rudolph *et al.*, Phys. Rev. C **65**, 034305-1 (2002).
33. H.T. Fortune, R.R. Betts, J.N. Bishop, M.N.I. Al-Jadir, R. Middleton, Nucl. Phys. A **294**, 208 (1976).
34. H. Röpke, J. Brenneisen, M. Lickert, Eur. Phys. J. A **14**, 159 (2002).
35. F. Brandolini *et al.*, Phys. Rev. C **64**, 044307 (2001).
36. Th. Andersson *et al.*, Eur. Phys. J. A **6**, 5 (1999).
37. N. Zeldes, A. Grill, A. Simieric, Mat.-Fys. Skr. Dan. Vidensk. Selsk. **3**, no. 5 (1967).
38. C.J. Chiara *et al.*, Phys. Rev. C **67**, 041303 (R) (2003).
39. C.J. Lister, A.M. Al-Naser, A.H. Behbehani, L.L. Green, P.J. Nolan, J.F. Sharpey-Schafer, J. Phys. G **6**, 619 (1980).
40. I. Lack *et al.*, Eur. Phys. J. A **16**, 309 (2003).
41. A.H. Behbehani, A.M. Al-Naser, C.J. Lister, P.J. Nolan, J.F. Sharpey-Schafer, Phys. Lett. B **74**, 219 (1978).
42. A.H. Behbehani *et al.*, J. Phys. G **5**, 1117 (1979).
43. P. Bednarczyk *et al.*, Eur. Phys. J. A **2**, 157 (1998).
44. J. Styczen, J. Chevallier, B. Haas, N. Schulz, P. Taras, M. Toulemonde, Nucl. Phys. A **262**, 317 (1976).
45. P.M. Endt, At. Data Nucl. Data Tables **55**, 171 (1993); **23**, 3 (1979).
46. T.W. Burrows, Nucl. Data Sheets **74**, 1 (1995).
47. G.D. Dracoulis, J.L. Durell, W. Gelletly, J. Phys. A **6**, 1772 (1973).
48. A.H. Wapstra, G. Audi, R. Hockstra, At. Data Tables **39**, 281 (1988).
49. C.L. Finck, J.P. Schiffer, Nucl. Phys. A **225**, 93 (1974).
50. N. Schulz, W.P. Alford, A. Jamshidi, Nucl. Phys. A **162**, 349 (1971).
51. W.P. Alford, R.A. Lindgren, D. Elmore, R.N. Boyd, Phys. Lett. B **46**, 356 (1973).

52. Kamal K. Seth, A. Saha, W. Benenson, W.A. Lanford, H. Nann, B.H. Wildenthal, Phys. Rev. Lett. **33**, 233 (1974).
53. C.W. Towsley, D. Cline, R.N. Horoshkov, Nucl. Phys. A **204**, 574 (1973).
54. W.J. Gerace, A.M. Green, Nucl. Phys. A **113**, 641 (1968).
55. C.R. Gruhn, T.Y.T. Kuo, C.J. Maggiore, H. McMann, F. Petrovich, B.M. Preedom, Phys. Rev. C **6**, 915 (1972).
56. S.W. Kikstra, C. van der Leun, P.M. Endt, J.G.L. Booten, A.G.M. van Hees, A.A. Wolters, Nucl. Phys. A **512**, 425 (1990).